TOPOGRAPHIC INFLUENCES ON WIND NEAR GREEN RIVER, UTAH

by

G. Hsi, G. J. Binder and J. E. Cermak

FLUID MECHANICS PROGRAM
ENGINEERING RESEARCH CENTER
COLLEGE OF ENGINEERING
COLORADO STATE UNIVERSITY
FORT COLLINS, COLORADO

Technical Report

TOPOGRAPHIC INFLUENCES ON WIND NEAR GREEN RIVER, UTAH

by

G. Hsi, G. J. Binder and J. E. Cermak

Distribution of this report is unlimited

Prepared under

U.S. Army Research Grant DA-AMC-28-043-65-G20
U.S. Army Materiel Command
Washington 25, D.C.

for

Atmospheric Science Office
Atmospheric Science Laboratory
White Sands Missile Range

Fluid Dynamics and Diffusion Laboratory
College of Engineering
Colorado State University
Fort Collins, Colorado

April 1968 CER67-68GH-GJB-JEC54

ABSTRACT

Actual terrain near Green River, Utah, was modeled to a scale of 1:800. The purpose of this study was to find the effect of topography on wind speed and wind direction.

Field data are included in this report and comparisons between model and prototype data are made.

Throughout this study, an ambient wind velocity of 4.57 mps was used and a neutral flow condition was maintained in the Army Meteorological Wind Tunnel.

TABLE OF CONTENTS

TABLE OF CONTENTS - Continued

LIST OF TABLES

LIST OF FIGURES

LIST OF FIGURES - Continued:

LIST OF SYMBOLS AND DEFINITIONS

Symbols

L	Height of meteorological tower (152.4 meters)
U	Local wind velocity, mps
U_a	Ambient wind velocity, mps
Z	Vertical distance from ground surface upward, meter
T	Location on model
P_1	Location on model
P_2	Location on model
P_3	Location on Model

Definitions

Level 1	1362.1 meter elevation prototype; 1.91 centimeters above model surface
Level 2	1377.4 meter elevation, prototype; 3.81 centimeters above model surface
Level 3	1392.6 meter elevation, prototype; 5.72 centimeters above model surface
Level 4	1407.9 meter elevation, prototype; 7.62 centimeters above model surface
Level 5	1426.8 meter elevation, prototype; 9.98 centimeters above model surface
Level 6	1446.9 meter elevation, prototype; 12.50 centimeters above model surface
Level 7	1471.9 meter elevation, prototype; 15.62 centimeters above model surface
Level 8	1499.3 meter elevation, prototype; 19.05 centimeters above model surface

Definitions (Continued)

Terrain characteristic map direction, angle β in degree

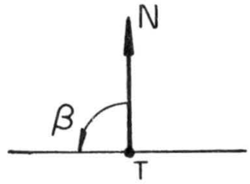

North direction of the model

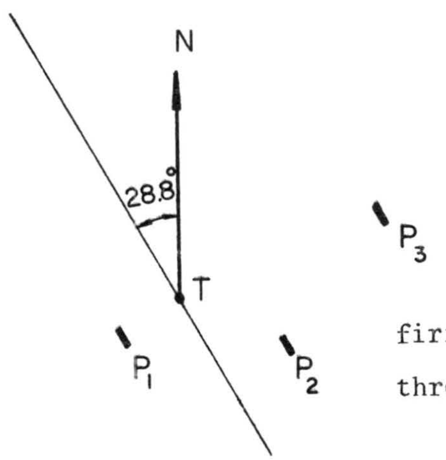

firing line (same for all three launch pads)

Ambient wind direction angle α (azimuth) in degree

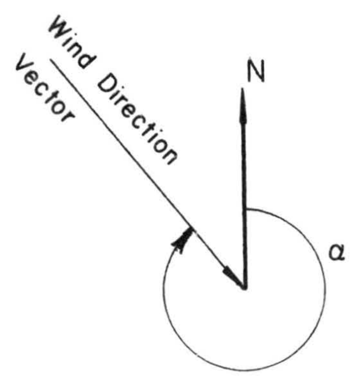

1. INTRODUCTION

The irregular topography of the earth's surface causes a lack of uniformity in wind structure which cannot be predicted from theory. The main concern of the work described in this report is the determination of wind speed profiles and wind direction variations from the ground surface up to 152.4 meters over a hilly area of 1524 meters in diameter. For this purpose, a model was built which simulated actual terrain near Green River, Utah.

The terrain modeled comprises the launching area for the United States Air Force - White Sands Missile Range multi-million dollar Athena missile re-entry project. The area selected includes three launch pads and the 150 m instrumented meteorological tower at the Green River Site. Wind velocity data were available from the Atmospheric Sciences Office 150 m tower. The basic operational problem is that of predicting airflow in the atmospheric boundary layer in the vicinity of the missile launch pads. The extremely uneven nature of the terrain at the Green River Site presents a unique challenge to simulate, in a wind tunnel, terrain-induced variations in the wind velocity profile of the boundary layer which can have a decided effect on missile ballistics.

The model was so constructed that it could be rotated in the wind tunnel, allowing a simulated ambient wind to pass over it from any direction. Four particular locations on the model were studied.

Throughout this study, uniform air density and zero pressure gradient were maintained in the Army Meteorological Wind Tunnel located in the Fluid Dynamics and Diffusion Laboratory, Engineering Research Center, Colorado State University. The ambient wind speed was 4.57 mps and the model scale was 1:800 in both the horizontal and vertical directions. Information was derived from photographs and aerial maps of the terrain under investigation for constructing the model. A special method for model construction was used to insure that every detail of the topography of the model was faithfully reproduced. The boundary-layer thickness of the approaching flow in the model was approximately scaled to the corresponding boundary-layer thickness for the prototype by placing the model at the downstream end of the long wind tunnel test section.

The region of the model flow most affected by topography was found to be the zone from the model surface up to 5.7 cm. A large portion of the wind-direction change and wind-speed reduction, and a high turbulence intensity were present in this zone. In checking the experimental reproducibility over such complex surface features of the model, less than 3% deviation was found in both the wind-speed profile and wind-direction variation.

To determine the viscous forces, or Reynolds number effect on the model, ambient wind speeds of 4.57, 9.15, and 18.30 mps were tested.

There was no noticeable change in the dimensionless velocity profiles with these variations of ambient wind speeds.

Of the three methods, namely, tufts, wind vane, and hot-wire anemometer (HWA), successively employed to measure wind direction, the hot-wire anemometer gave the most accurate and reliable data. The greatest effect of model terrain on the ambient wind direction was 5.6°, which was sensed by the HWA and occurred at an ambient wind azimuth of 30°.

This report includes both field and laboratory data. However, only mean velocity data with no corresponding temperature data were available from the field so that critical comparison of model and field data was not possible. A constant effort to compare actual field data with laboratory data is necessary in order to provide an established basis for determining the degree of simulation for such topographic model studies.

2. MODELING TECHNIQUE

2.1 Atmospheric Similarity Considerations

In order to complete atmospheric flow similarity in two systems of different length scales, geometrical, dynamic, and thermal similarity must be achieved as shown in Reference 1. However, the requirement of identity of the equations of motion and energy for the two systems usually can be met only in an approximate sense. In this study, geometrical similarity was maintained for the best approximation in mean wind speed profiles and mean wind direction variations over the specified topographic area. A neutral flow condition was also maintained in the wind tunnel to eliminate stratification of air density and, thereby, to simplify the study.

Accordingly, all criteria for similarity required by conservation of energy were satisfied for neutral atmospheric flow. However, the Reynolds number criteria (UL/ν) required by conservation of momentum (equation of motion) is not strictly satisfied. Because of the 1:800 scale the ratio of model to prototype Reynolds numbers was about 1:800 since the model wind speeds and fluid viscosity were essentially equal to those for the prototype. Because of the sharp topographic features this inequality of Reynolds numbers was not considered to be a serious limitation in meeting the objectives of this study.

2.2 Topographic Characteristics

The terrain characteristics were mapped by drawing radial lines from the center of the investigated area to the edge of an aerial map and noting the points at which these radial lines crossed elevation lines. Figure 7 shows the terrain characteristics and Fig. 6a shows the area which was actually modeled. The wind-tunnel testing section width determined the scale of the model for the particular topographic area of interest -- 1:800. The most significant fact to be observed from these sections is that the terrain has rather sharp changes in slope as one passes across the area. From the modeling point of view this is important since the breaks in slope will control the local flow patterns. This means that geometrical features, i.e., local pressure gradients, control the flow and not the viscous forces. Accordingly, the discrepancy between model and prototype Reynolds numbers does not have serious consequences in regard to attainment of flow similarity.

3. MODEL CONSTRUCTION

3.1 Filling Method

For studies of meso-scale phenomena in the atmosphere, the area to be investigated is usually large. Therefore, the length scale must be greatly reduced. The largest possible model is always favored because of Reynolds number requirements. The final decision on the modeling scale to be used is always a compromise between the size of the wind tunnel test section and the smallest extent of the area to be studied which will still include the important topographic characteristics.

From such considerations, the scale factor of the proposed model was decided, and the area of the aerial map to be investigated was photographically enlarged or reduced to fit the area of the model base. In the case of the study under discussion, there was no preference of wind direction, so a circular base was adopted for its convenience for rotation in the wind tunnel to vary the approaching wind direction. The photographically scaled map was then glued to the 1.27 cm plywood base.

On the map contour lines are clearly shown. To establish these contours on the model, 0.0305 cm thick aluminum strips of the appropriate widths were mounted vertically along these contour lines.

To fill the space between the contour line sheets, polyurethane duo-foam was poured into place, and parts higher than the contour line strips were trimmed away.

This procedure offers several advantages: at this stage, the model is very light, and can withstand temperatures up to 94°C without deformation of the polyurethane duo-foam, and construction time up to this point is very small. This method allows most of the construction time to be spent on finishing the surface of the model, which is the important feature under investigation.

In the next step, putty was applied to the surface of the model to furnish a smooth surface and match details of the terrain between contour lines. After the putty had dried, it was smoothed with sandpaper. Final steps, such as roughening the model surface, marking out roads, and placing model buildings, were then taken. Photographs of the completed model are shown in Figs. 9 and 10.

3.2 Placement of Model in the Wind Tunnel

The model was 1.9 m in diameter and was placed at the center position of the wind-tunnel floor. Because the area studied was surrounded by irregularly-shaped mountains and hills, a layer of 1.27 cm diameter gravel was placed around the model's circumference, as shown in Fig. 6. This graveled region had two notable effects: it raised the roughness to approximately that of the prototype, and it prevented separation of flow at the edge of the model. The arrangement of the model in the wind tunnel is shown in Fig. 6.

4. EXPERIMENTAL TECHNIQUES

4.1 Mean Wind Speed Measurement

A Prandtl tube was used to measure the mean wind velocity. Readout was made from a Trnas-sonic pressure meter. Because of high turbulence intensity at the near surface region of the model, a digital voltmeter was connected to the Trans-sonic pressure meter. From the digital voltmeter, ten sample readings were taken for averaging and for arriving at the mean wind speed.

4.2 Mean Wind Direction Measurement

Three techniques for measuring mean wind direction were successively tried during this study. Of the three (tufts, wind vane, and hot-wire anemometer) the hot-wire anemometer gave the most satisfactory results, although its use was very time consuming.

One of the pressing needs for this type of wind-tunnel study is the development of a simple and accurate mean wind direction sensor. An accurate and convenient instrument for this purpose when low wind speeds are employed must emphasize some principle not currently in use for this function.

4.2.1 Tuft method - Although shifting of the mean wind direction could be sensed by use of wool tufts, the angle reading was neither obvious nor exact, as can be seen from Fig. 11. Because of the rigorous nature of this study, this type of wind direction measurement was discarded.

4.2.2 Wind-vane method - After the effort to use a tuft technique, efforts were made to develop a small wind vane for the measurement of wind direction over the model. An ultra-low torque potentiometer was used to sense the angle change of the vane.

At low wind speeds, in the vicinity of 4.57 mps, the wind vane motion was impeded by friction until a small buzzer was attached to the potentiometer on which the wind vane was mounted. With this improvement the accuracy of the reading depended heavily on the degree of induced vibration at velocities below 3.05 mps. A critical factor was found to be the accurate balance of the vane itself.

Figure 12 shows the change in angle of the vane at a specific location over the model in an airstream with a speed of 9.15 mps. Although field data show direction changes in this location as great as 15^{o}, the direction changes, as can be seen from Fig. 12, amount to only about 2^{o}. Level heights for model and prototype are given under Definitions, p. vii.

This discrepancy reflects two facts: high wind velocity over the model straightens the wind vane and overshadows the terrain effect, and there is a major difference in wind orientation influence between the actual terrain and the transition area in the model. That is, wind direction changes have already taken place over the actual terrain before the wind reaches the area under study, while in the wind tunnel these direction changes begin only at the edge of the model.

4.2.3 Hot-wire method - It is well known that the rate of heat transfer from an electrically heated wire bears a direct relationship to its angle of yaw relative to the direction of airflow. Specifically, the heat transfer is maximum when the hot wire is perpendicular to the direction of airflow, and it is minimum when the hot wire is parallel to the direction of airflow.

Determination of the mean wind direction, then, can be accomplished by rotating the hot-wire anemometer in a horizontal plane and plotting the output versus the angle. The minimum value on this curve defines the mean wind direction. Since the curve is symmetrical about the minimum value, it should be sufficient to determine the angles of two positions giving the same output. The average of these two angles corresponds to the minimum. To permit an immediate check of the angle measurement, the output for only two pairs of points is taken.

The hot-wire anemometer probe is mounted on a rotating actuator geared to a potentiometer for remote angle reading. This actuator is mounted on the vertical positioner of the probe. Next, the output is "bucked out" with a stable power supply with fine control. The fluctuations of this modified output due to turbulence are damped with a 2,000 μf capacitor.

Data were obtained from twelve runs corresponding to twelve free-stream wind directions 30° apart. For each free-stream wind direction, four specified points, labeled T , P_1 , P_2 and P_3 were investigated, and for each specified point, wind directions at eight vertical levels, the highest corresponding to 152.4 m above the ground level of the prototype, were recorded.

5. EQUIPMENT

5.1 Meteorological Wind Tunnel

The meteorological wind tunnel (Ref. 8) at the Colorado State University Fluid Dynamics and Diffusion Laboratory employs a test section 27 m long and a nominal cross-sectional area of 4 m^2 which can be adjusted for establishing negative and positive pressure gradients (see Table I). A large contraction ratio of 9:1 in conjunction with a set of four damping screens yields an ambient turbulence level of about 0.1 per cent.

The tunnel can be used for either closed or open loop operations. Test-section air velocities range from 0 to about 37 mps, and the ambient temperature of the air can be varied from 0°C to 85°C at medium speeds. In addition, the humidity of the ambient air can be controlled. In the test-section floor, the tunnel has a 12.2 m section which can be heated or cooled to permit temperature differences between the cold plate and hot air of 65°C and between the hot plate and cold air of more than 105°C.

A carriage system is available which permits remote placement of probes. Instrumentation associated with the facility consists of a complete system for sensing, analyzing, and recording turbulence and for determining the mean value of velocity, temperature, and concentration (mean values only). Performance characteristics of the Meteorological Wind Tunnel are listed in Table 1.

5.2 Instruments

The hot wire was 0.000508 cm in diameter and 0.127 cm in length with a resistance of 5 ohms. A Disa hot-wire probe, 55-A type, was used with a Disa constant temperature anemometer.

A 2000 μf capacitor was used for slowing the turbulence fluctuation output. A Hewlett 340-A digital voltmeter with a range of 0.1 mv to 1000 v was adopted for accurate voltage readings. To stabilize the bucking system for wind-direction measurements, a DC power supply was used. An x-y plotter was also used for wind-direction measurement.

For mean wind speed measurements a 0.317 cm diameter Prandtl tube and an equibar pressure meter, Trans-sonic, Inc. type 120, were used.

6. TESTING PROCEDURES

6.1 Mean Wind Velocity

To measure a fixed ambient wind velocity, the 0.318 cm diameter Prandtl tube was set at level 1, over one of reference points, say T, on the model. The output was then fed to an equibar pressure meter, from which the signal was transferred to a digital voltmeter. Because of the turbulence fluctuation, a mean velocity speed was obtained by averaging ten readings from the digital voltmeter. Then, by use of the remote actuator, the Prandtl tube was moved to level 2 for another reading. After readings at eight levels were recorded, the actuator was then moved to the next reference point, say, P_1, for eight more readings.

In this way, each of the points T, P_1, P_2, and P_3 were investigated for each fixed ambient wind direction.

6.2 Mean Wind Direction and Ambient Wind Direction

To determine mean wind direction, the hot-wire probe was first set in the free ambient stream, that is, at the mid-height of the wind tunnel, 0.9 meter above the tunnel floor. The hot wire was in the plane parallel to the tunnel floor and also parallel to the free ambient stream. This position allowed the hot wire to pick the minimum readout. Then, by rotating the hot wire along each side of a 15 degree angle, the millivolts versus angle calibration curve was obtained. At the minimum readout point from the calibration curve, the direction of ambient wind, or the reference direction could be obtained. Finally, the hot-wire probe was lowered to level eight which is over a specified point, say T, for the wind direction measurement over the model at that point.

The signal of varying millivolts due to hot-wire angle change was translated by an x-y plotter. This was an easy way to decide if the hot wire was at minimum readout position, or the mean wind direction. For adjusting the voltage output of the hot wire, a bucking device was used to reduce the voltage output to a range such that the x-y plotter could be set at 50 mv/div scale in order to get more accurate results.

The hot wire was then lowered to each of the eight levels indicated by location of measurements in the field. At each level a graph was obtained through use of the x-y plotter simply by rotating the hot wire 30 degrees and putting the minimum readout at the center of the graph.

For the purpose of avoiding the time lag of the instrument, discrete point plotting was used. First, two points on each side of the linear slope were printed. They provided a good and clear way to obtain the minimum readout position on the graph. It should be kept in mind that the counterpart points should be printed on the same level on the graph if an accurate result is expected.

After nine readouts, one for each level and one for ambient wind, the wind direction change over one point of the model, say T , was clearly obtained. According to the calibration of the actuator with no model in the wind tunnel, the accuracy for wind direction was ± 0.5 degrees.

7. EXPERIMENTAL RESULTS

7.1 Mean Wind Speed Profiles

The ambient wind speed was 4.57 mps for all data. Twelve ambient wind azimuths were tested over the topographic model.

In general, the model terrain had influence on the wind speed from the model surface up to the elevation of level eight over the four positions T , P_1 , P_2 , and P_3 . All the wind speed profiles follow closely the 1/7th power distribution which was based on a boundary-layer thickness of 0.495 m over the tower site and the equation

$$\frac{U}{U_a} = \left(\frac{z}{\delta}\right)^{1/7} . \qquad (7.1)$$

Wind speed profiles are shown from Figs. 16 to 27. A comparison of the elevations of the four sites shows that P_2 is the highest and T is the lowest, P_1 and P_3 are at the same elevation but separated by a small hill. Because of the elevation difference, P_2 had the largest U/U_a value at level one except for α equal to 90^o, 120^o and 300^o; T had the lowest value in U/U_a at level one except for α equal to 0^o and 30^o, P_1 and P_3 had U/U_a values between those for P_2 and T The exceptions were due mainly to the local terrain features close to the site studied. At level one, the maximum U/U_a was 0.82 which happened at P_2 for α equal to 240^o, and the minimum U/U_a was 0.54 at tower site for $\alpha = 270^o$. At level eight, the maximum U/U_a was 0.975 at P_3 for $\alpha = 180^o$, the minimum was 0.82 at P_1 and P_2 for $\alpha = 90^o$, and T_1 and P_1 at $\alpha = 300^o$.

The influence of the upstream condition on wind speed profiles were compared as follows:

(i) 0^o wind azimuth: uphill condition

Site T had a U/U_a value larger than that of P_1 and P_3 for all eight levels and also larger than that of P_2 from level four upward. This was because the wind passed a long valley and was toward T . However, P_2 was at a higher elevation, and hence had a U/U_a value larger than that of T up to level four.

(ii) 30^o, 60^o and 90^o wind azimuths: gentle uphill condition

For 30^o wind azimuth, the wind speed profiles followed closely the 1/7th power distribution over the four sites, particularly from level five upward. For 60^o and 90^o wind azimuth, almost the same upstream condition existed. T and P_1 sites had the same wind speed profiles for 60^o wind azimuth.

(iii) 120^o, 150^o, 180^o, 210^o, and 240^o wind azimuths: uphill condition, over a 60 m high cliff, then downhill condition

For 120^o wind azimuth, the wind was tangent to the cliff before reaching sites T, P_1 and P_2. P_3 had a flat uphill slope and had less influence from the cliff. P_3 had larger U/U_a than T, P_1 and P_2. For 150^o wind azimuth, P_1 and P_2 had the same wind speed profiles. For 180^o wind azimuth, the ambient wind direction was perpendicular to the cliff. The cliff had the larger influence on P_2 and P_3 from level five upward. For 210^o and 240^o wind azimuth, P_2 had the largest U/U_a value among T, P_1 and P_3. As to T, P_1 and P_3, their wind speed profiles followed 1/7th power distribution from level four upward.

(iv) 270^o and 300^o wind azimuths: flat upstream condition

For 270^o wind azimuth, the wind speed profiles followed one another closely for P_1, P_2 and P_3. T had U/U_a smaller than the rest. For 300^o wind azimuth, T and P_1 were on the same line perpendicular to the ambient wind direction, they had the same wind speed profiles.

(v) 330^o wind azimuth: uphill condition

T and P_1 had about the same wind speed profiles. P_2 had the largest U/U_a value. Because of the fact that the atmospheric boundary-layer thickness varies from time to time and the flow condition is affected by changes such as temperature, eddy viscosity, etc., the experimental data can serve only as a reference for the field data. It is clearly understood that the experimental data represent steady, neutral flow conditions most accurately.

7.2 Mean Wind Direction Profiles

As for mean wind speed study, the ambient wind was 4.57 mps for examining the wind direction changes over the four sites T, P_1, P_2 and P_3 of the model. Twelve wind azimuths were investigated. Large wind direction changes were shown from level one up to level four for all four sites. These were produced by the influence of local terrain features. Mild changes were observed from level five upward. Data are shown in Figs. 16 to 27. A combined wind direction variation over the tower site is plotted in Fig. 15.

For 0^o, 30^o and 60^o wind azimuth, the wind directions turned in a counterclockwise direction over the site. By looking into the upstream flow condition the approaching flow was up a gentle uphill slope from an elevation of about 1320 m to an elevation of 1350 m near the sites, but there was higher terrain near the sites to the west and southwest. Thus, the flow was forced to turn in the counterclockwise direction. The biggest direction change detected by the HWA was about 5.6^o at the tower site and P_1 at level one for 30^o wind azimuth.

For 120^o, 150^o and 180^o wind azimuths, the flow passed over a steep 60 m high cliff before reaching the sites. According to wind directions recorded by the HWA, there was a clockwise turning tendency for the flow over these four sites. The flow approaching the sites was from a southeast direction over the cliff. For 210^o and 240^o wind azimuth, the flow was from about the soutwest direction, passing over the high cliff and then onto the sites. The flow had a counterclockwise sense over the sites. For 90° and 330° wind azimuths, there were similar wind direction changes over T, P_1 and P_3, but it was different for P_2. For 270° and 300° wind azimuths, the flow was over a flat hilly upstream condition. The flow directions were influenced more by local feature of the terrain than by the distant terrain, as are shown in Figs. 25 and 26.

7.3 Field Wind Speed Profiles

Wind speed profiles averaged over 180 seconds and 300 seconds were recorded in the field at the tower site. These two profiles were taken on July 1 and on July 16, 1965, respectively. One profile showed a wind velocity of 1.89 mps at level one and 5.81 mps at level eight. The other profile had a 3.78 mps wind at level one and a 6.04 mps wind at level eight (see Figs. 28 and 28.a). According to the wind azimuth of the field data, a wind speed profile over the tower site of the model was selected and plotted on the graphs.

In order to compare experimental and field data, wind velocity at level eight was chosen as the characteristic velocity for the experimental data -- the smoothed field data curve was plotted and used as the dimensionless field velocity profile. Figure 28 shows a good agreement between model and prototype. However, the data shown in Fig. 28a are in poor agreement. Hence, more field data are needed to better understand the nature of the field flow and to provide an explanation why good agreement between field and laboratory data is not good for both of the cases which were compared.

7.4 Field Wind Direction Profiles

Figure 29 shows the field wind azimuths 102° at level four and 119.5° at level eight. Figure 29a shows the field wind azimuths 156° at level one and 183.5° at level six.

Adopting the field wind azimuths, experimental wind direction profiles over the tower site of the model were plotted on the graphs. The field wind direction was influenced by Coriolis acceleration, but the experimental data had no such influence; therefore, an amount of wind azimuth change due to the Coriolis was subtracted from the field data which was calculated as follows (see reference 7).

By assuming that vertical velocity component and the horizontal variations of the horizontal velocity components can be neglected, the equation of motion for a viscous fluid are

$$\frac{\partial u}{\partial t} + u\frac{\partial u}{\partial x} + v\frac{\partial u}{\partial y} - 2\omega \sin\phi\, v = -\frac{1}{\rho}\frac{\partial p}{\partial x} + \frac{1}{\rho}\frac{\partial}{\partial z}\left(\mu\frac{\partial u}{\partial z}\right) \tag{7.2}$$

$$\frac{\partial v}{\partial t} + u\frac{\partial v}{\partial x} + v\frac{\partial v}{\partial y} + 2\omega \sin\phi\, u = -\frac{1}{\rho}\frac{\partial p}{\partial y} + \frac{1}{\rho}\frac{\partial}{\partial z}\left(\mu\frac{\partial v}{\partial z}\right) \tag{7.3}$$

When the wind distribution above the surface layer is studied, the pressure-gradient force and Coriolis force are taken into account. Assume that the pressure gradient is independent of the altitude, that the isobars are parallel straight lines, and that the motion is horizontal and steady, the motion would then be geostrophic except for the influence of eddy and molecular viscosity. If μ is assumed to be constant and x-axis is oriented parallel to the pressure gradient, the equation of motion becomes

$$-2\omega \sin \phi \; v = - \frac{1}{\rho}\frac{\partial P}{\partial x} + \frac{\mu}{\rho}\frac{d^2 u}{dz^2} \tag{7.4}$$

$$2\omega \sin \phi \; u = \frac{\mu}{\rho}\frac{d^2 v}{dz^2} \; . \tag{7.5}$$

The following expressions of the solutions are used to solve the equations of motion

$$u = - A \, v_g e^{-az} \sin (az - b) \tag{7.6}$$

$$v - v_g = B \, v_g \, e^{-az} \cos (az - b) \tag{7.7}$$

where the geostrophic wind speed v_g is

$$v_g = \frac{1}{2\omega \sin \phi} \frac{1}{\rho}\frac{\partial p}{\partial x} \; , \text{ a constant} \tag{7.8}$$

and A, B, a and b are constants.

After differentiating Eqs. (7.6 and 7.7) twice and substituting into Eqs. (7.4 and 7.5), the following relation can be obtained

$$B = - A \tag{7.9}$$

$$a = \sqrt{\frac{\rho\omega \sin \phi}{\mu}} \tag{7.10}$$

thus

$$u = - A \, v_g \, e^{-az} \sin (az - b) \tag{7.11}$$

$$v = v_g \, [1 - A \, e^{-az} \cos (az - b)] \tag{7.12}$$

constants A and b are found from the boundary conditions $z = z_a = 0$

$$b = \frac{\pi}{4} - \alpha_o \tag{7.13}$$

$$A^2 = 2 \cos^2 \alpha_o \tag{7.14}$$

where

$$\alpha_o = \tan^{-1} (1 + 2 \kappa a) \tag{7.15}$$

and

$$\kappa = (z_a + z_o) \ln \left(\frac{z_a + z_o}{z_o} \right) . \tag{7.16}$$

The solutions are

$$u = - v_g \sqrt{2} \cos \alpha_o e^{-az} \sin (az + \alpha_o - \frac{\pi}{4}) \tag{7.17}$$

$$v = v_g [1 - \sqrt{2} \cos \alpha_o e^{-az} \cos (az + \alpha_o - \frac{\pi}{4}) \tag{7.18}$$

The following data were assumed to calculate the wind direction change over Green River:

The latitude of Green River $\phi = 38^o$
The coefficient of surface friction $\kappa = 55.2$ m
Geostrophic wind speed = 6 mps
Eddy viscosity = 110 gm cm^{-1} sec^{-1}
Air density at elevation 1220 m = 1.1×10^{-3} gm cm^{-3}
The angular velocity of the earth rotation $\omega = 7.292 \times 10^{-5}$ sec^{-1}
The roughness parameter $z_o = 4$ cm
The shear of the wind is parallel to the wind itself at level $z_a = 10$ m.

It was found that the wind direction change due to the Coriolis force effect was 5.3° at level eight (see Fig. 29b). α_o and eddy viscosity will change widely, depending on the weather situation and on the nature of the surface of the earth; therefore, the calculated correction is subject to considerable error. However, both data show about the same tendency of curve variation from level one to level eight.

7.5 Boundary-Layer Thickness over the Model Tower Site

It was found that the boundary layer thickness at the tower site was 0.495 m measured from the model surface. The model was set at 330°, and the ambient wind velocity was 9.14 mps. Figure 30 shows the boundary-layer profile.

7.6 Reproducibility of the Wind Velocity Profile

Figure 31 shows three independent runs over the tower site. The overall reproducibilities were well matched at levels 1, 2, 4, 7 and 8. At level 2, 0.04 U/U_a was the difference between datum one and datum two.

7.7 Reynolds Number Effect on the Model

Ambient wind speeds of 4.57, 9.15 and 18.30 mps were used and wind speed profiles were taken at the tower site for α equal to zero degree. There was found to be no change in the dimensionless velocity profiles. Thus, the viscous force or the Reynolds number was not a dominating factor for this study.

7.8 Reproducibility of Wind Direction Variations

The reproducibility of wind direction variations was first checked at a fixed point in the free stream (low turbulence) and proved to be less than 0.2^{o} when measured by use of the hot-wire anemometer method. During actual measurements, the hot-wire anemometer had to be moved up and down with the vertical actuator. Small bumps on the rails on which the carriage was moving could have led to faulty angle readings. In order to prevent this, the probe was raised and lowered in the unobstructed tunnel. After measurement, the wind direction was found to be constantly within 0.3^{o}. Finally, three independent runs were made over the tower site to check the overall reproducibility. These measurements are plotted in Fig. 33. It can be seen that the discrepancies among the three measurements at a given point are on the average less than 0.3^{o}. Only at the lowest level is there a larger deviation of 0.75^{o} which may be attributed to the high degree of turbulence there.

8. CONCLUSIONS

(a) The mean wind speed profiles over the model were compared with the 1/7th power profile for all twelve wind azimuths studied in the model. These profiles were found to be essentially similar to the 1/7th power profile.

(b) Model wind speed profiles can be used to interpret field wind speed profiles provided the reference wind speeds used in the dimensionless wind speed plots are taken at corresponding heights.

(c) The wind directions of the field data and the model data have the same tendency from ground up to level five. The field wind direction change, after subtracting the Coriolis force effect, can be close to the experimental data provided more information of the field is recorded (see section 7.4).

(d) The model scale 1:800 is proper for the mean wind speed study. For the wind direction study a larger model scale ratio is desirable; however, if a satisfactory area coverage is to be maintained, a larger wind tunnel would be required.

(e) The hot-wire anemometer (HWA) method employed to measure wind directions over the model is better than the tufts method and the wind vane method.

(f) A continuous effort to compare field and experimental wind data is needed to improve our understanding of model-prototype relationships.

(g) From the results of the Green River simulation experiment, it is apparent that the salient features of terrain-induced variations in airflow can be resolved. While differences are less pronounced for the model because of the small scale involved, the efficacy of the simulation approach appears to remain intact, which suggests the desirability of further investigations of this nature in the controlled environment of a meteorological wind tunnel.

BIBLIOGRAPHY

1. Blackadar, A. K., The Vertical Distribution of Wind and Turbulent Exchange in a Neutral Atmosphere. J. of Geophysical Research Vol. 67, No. 8, July 1962.

2. Estoque, M. A., An Approximation to Boundary Layer Wind Profiles. Hawaii Institute of Geophysics, University of Hawaii, November 1965.

3. Cermak, J. E., V. A. Sandborn, E. J. Plate, G. J. Binder, H. Chuang, R. N. Meroney and S. Ito, Simulation of Atmospheric Motion by Wind-Tunnel Flows. CER66-JEC-VAS-EJP-GJB-HC-RNM-SI-17, Colorado State University, May 1966.

4. Cermak, J. E., and J. A. Peterka, Simulation of Wind Fields over Point Arguello, California, by Wind Tunnel Flow over a Topographical Model. Final Report U.S. Navy Contract N126(61756)34361A(PMR). Fluid Dynamics and Diffusion Laboratory report CER65JEC-JAP64, Colorado State University, December 1965.

5. Cermak, J. E., and R. N. Meroney, Wind Tunnel Models of Flow and Diffusion over San Nicolas Island. Progress Report for 4th and 5th quarters on Contract N123(61750)50192A(PMR), November 1965.

6. Delleur, J. W., Flow Direction Measurement with Hot-Wire Anemometers. Hydraulics Division Conference, ASCE, Tucson, Arizona, August 1965.

7. Haurwitz, B., Dynamic Meteorology. McGraw-Hill, New York, 1941.

8. Plate, E. J., and J. E. Cermak, Micrometeorological Wind Tunnel Facility. Fluid Dynamics and Diffusion Laboratory Report CER63EJP-JEC9, Colorado State University, February 1963.

APPENDIX

TABLE AND FIGURES

TABLE 1. PERFORMANCE CHARACTERISTICS OF THE METEOROLOGICAL WIND TUNNEL

Characteristic	Meteorological Wind Tunnel
1. Dimensions	
Test-section length	27 m
Test-section area	3.4 m^2
Contraction ratio	9.1
Length of temperature controlled boundary	12 m
2. Wind-Tunnel Drive	
Total power	200 kw
Type of drive	4-blade propeller
Speed control: coarse	Ward-Leonard DC control
Speed control: fine	Pitch control
3. Temperatures	
Ambient air temperature	$5^{\circ}C$ to $95^{\circ}C$
Temp. of controlled boundary	$5^{\circ}C$ to $205^{\circ}C$
4. Velocities	
Mean velocity	Approx. 0 mps to 37 mps
Boundary layers	up to 50 cm
Turbulence level	About 0.1 per cent
5. Pressures	Adjustable gradients
6. Humidity	Controlled from approx. 20% to 80% relative humidity under average ambient conditions

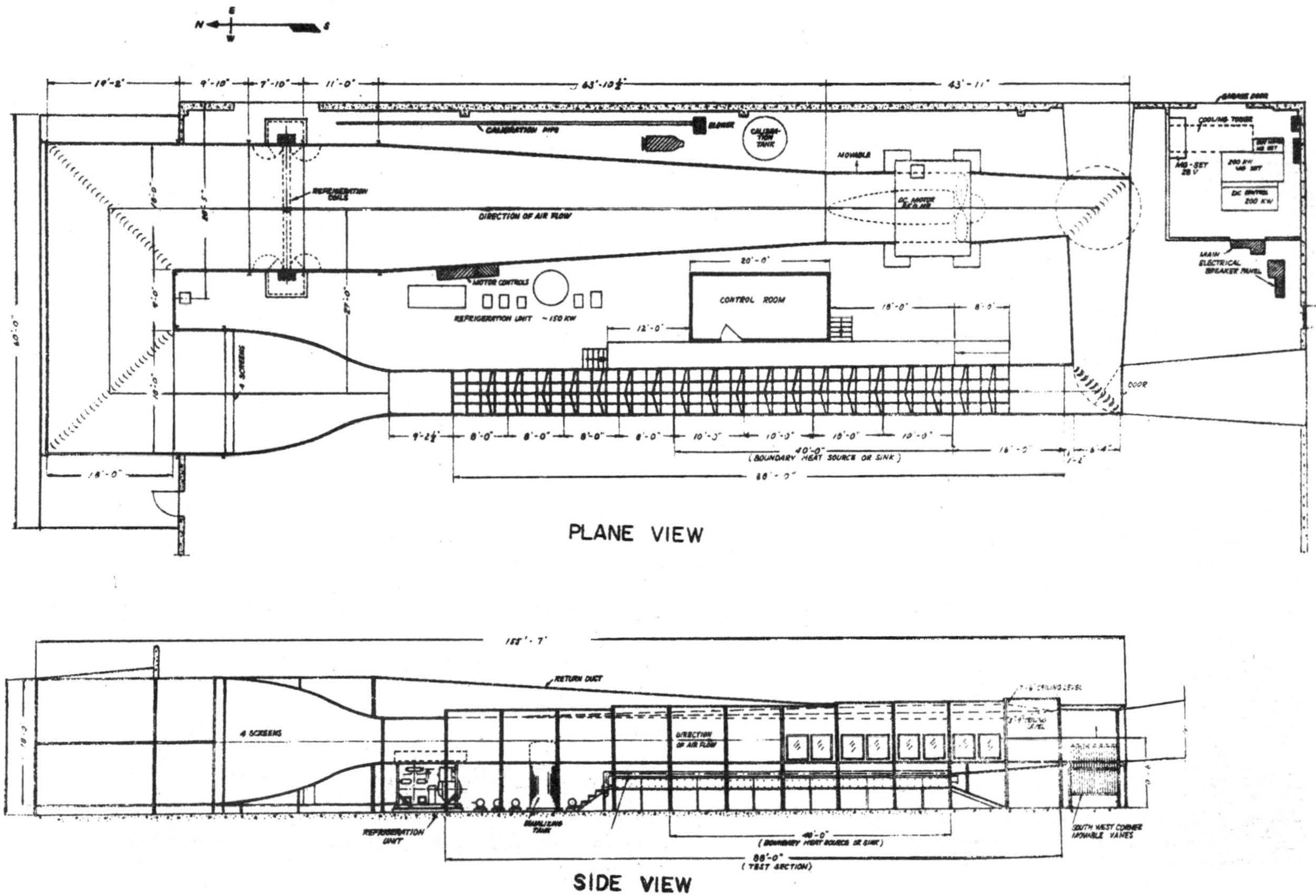

Fig. 1 Army meteorological wind tunnel

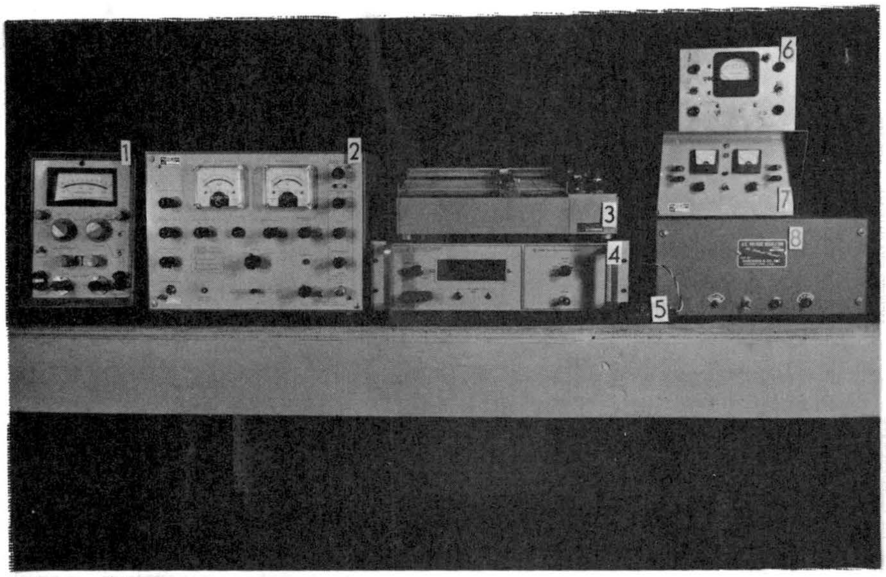

Fig. 2 Instruments

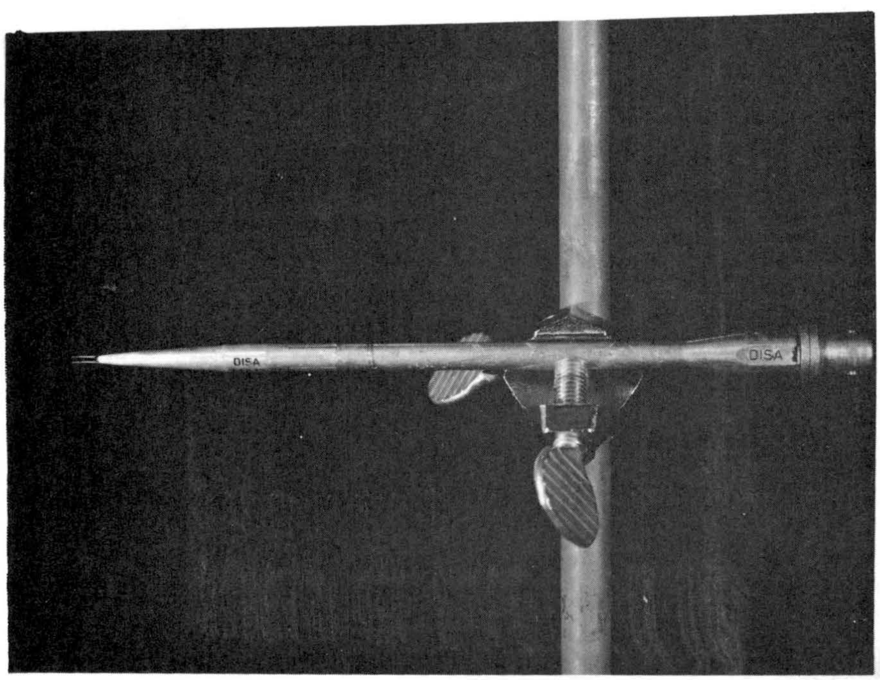

Fig. 3 Hot-wire and Disa probe

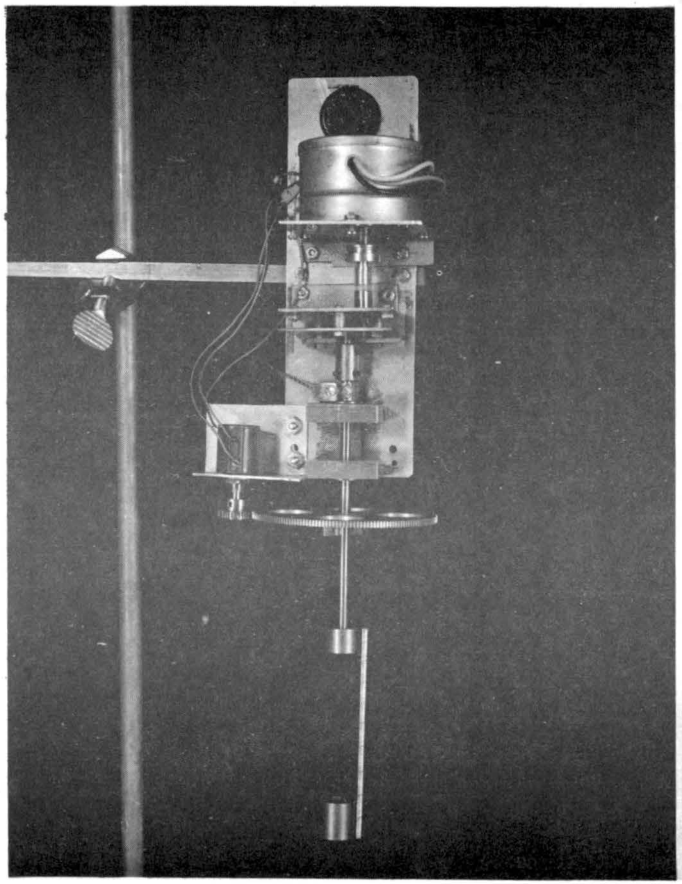

Fig. 4 Rotator

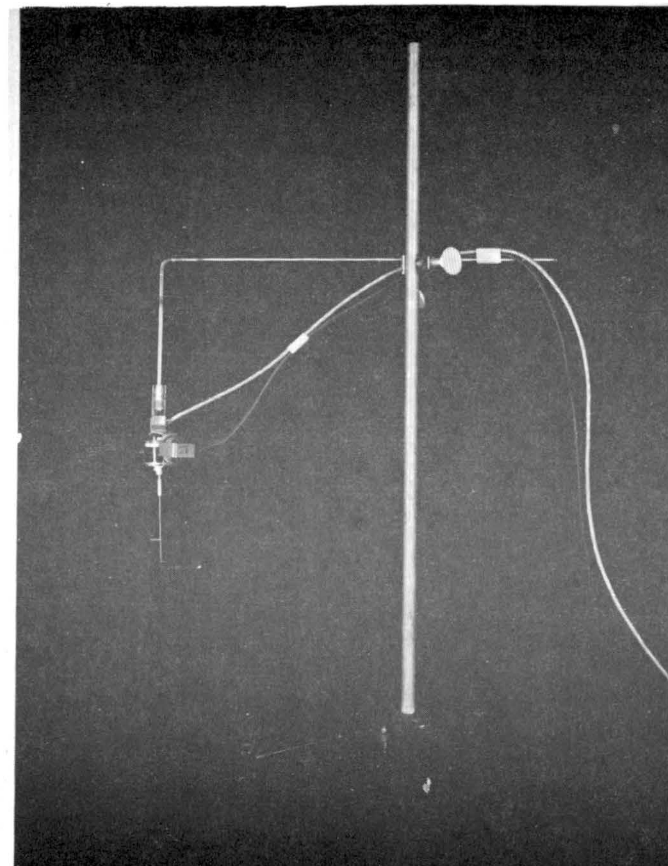

Fig. 5 Wind vane and vibrator

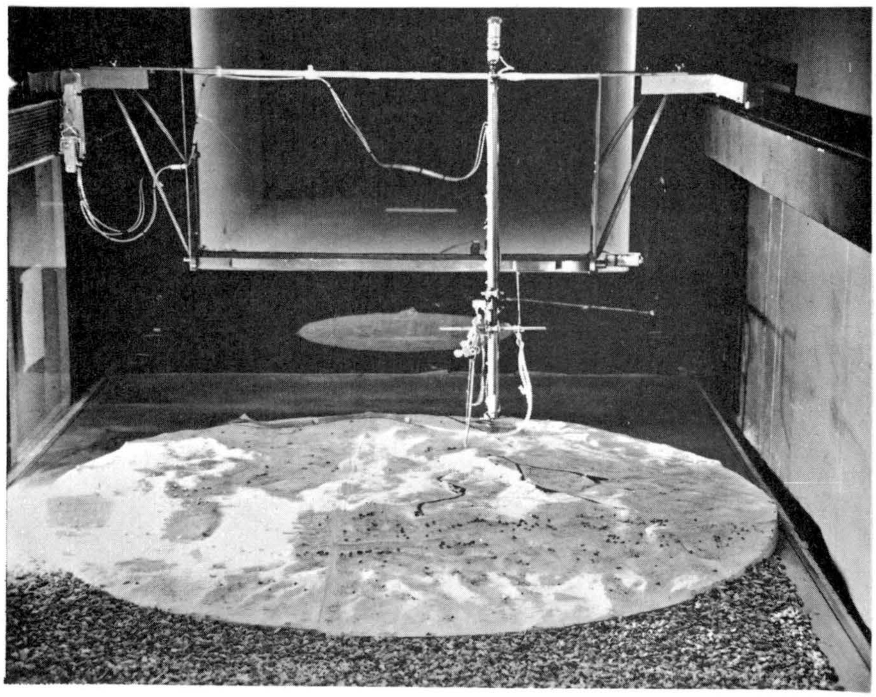

Fig. 6 Model in the meteorological wind tunnel

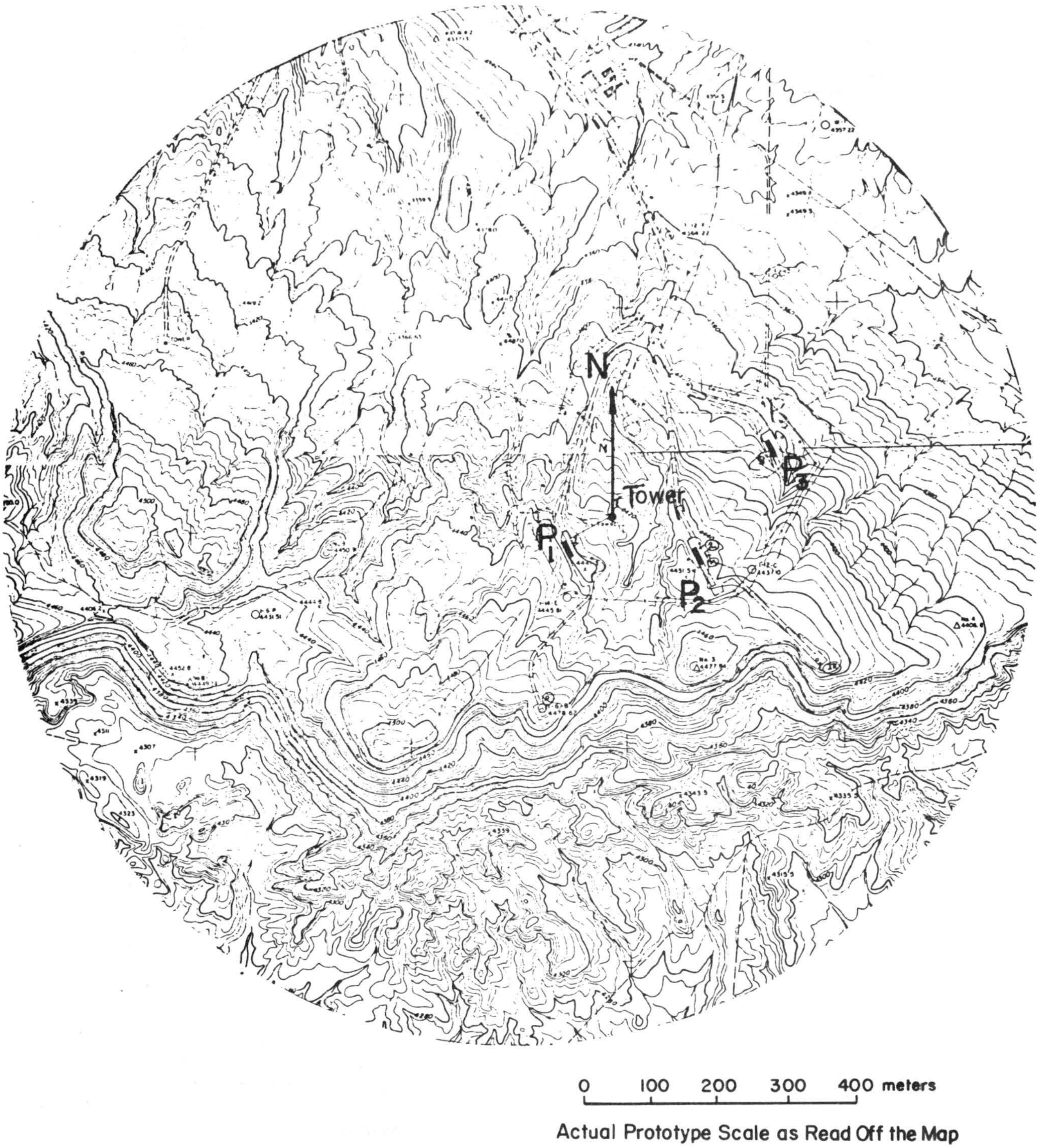

Fig. 6a The model feature of Green River terrain

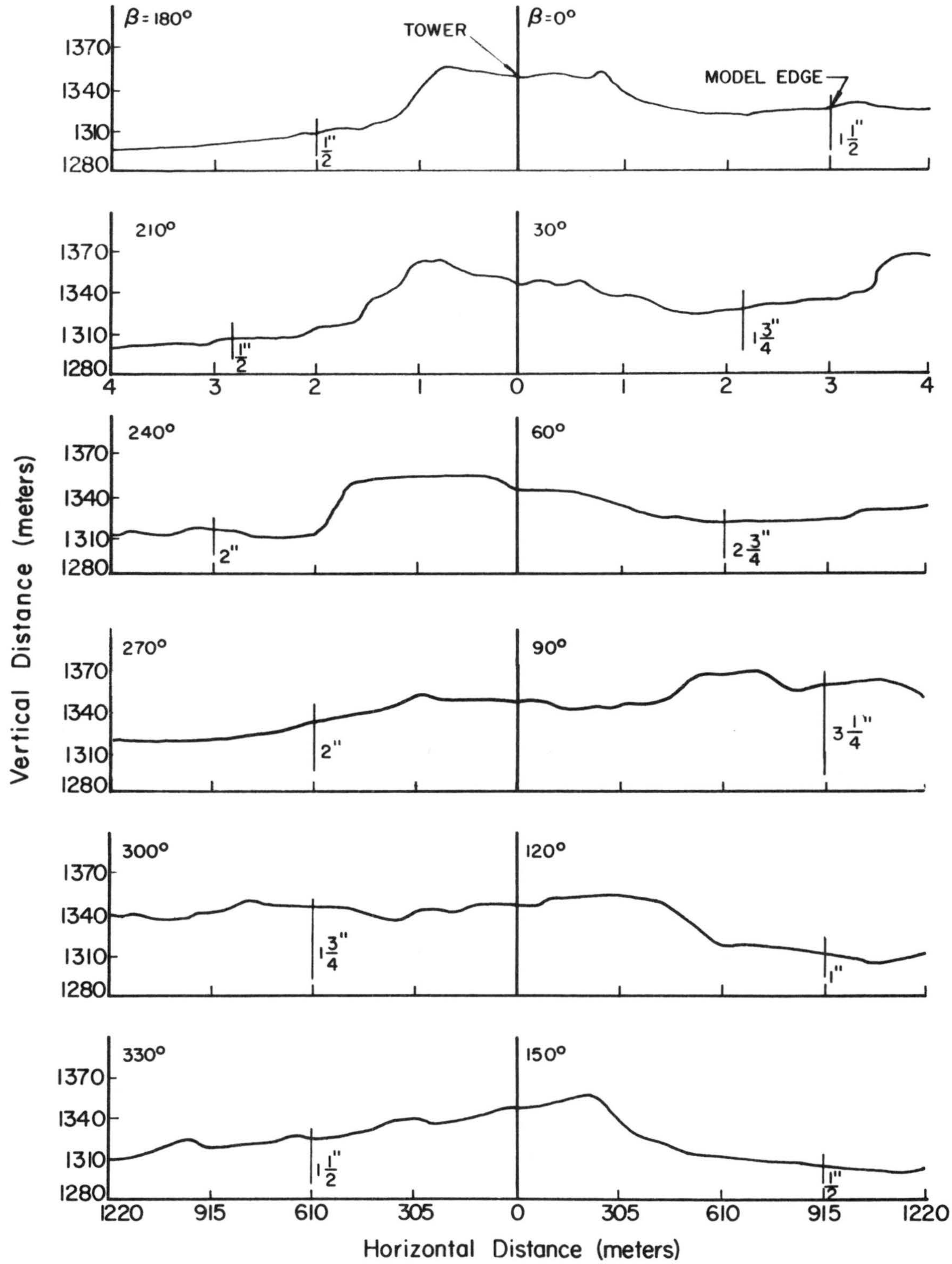

Fig. 7 Green River field terrain characteristics

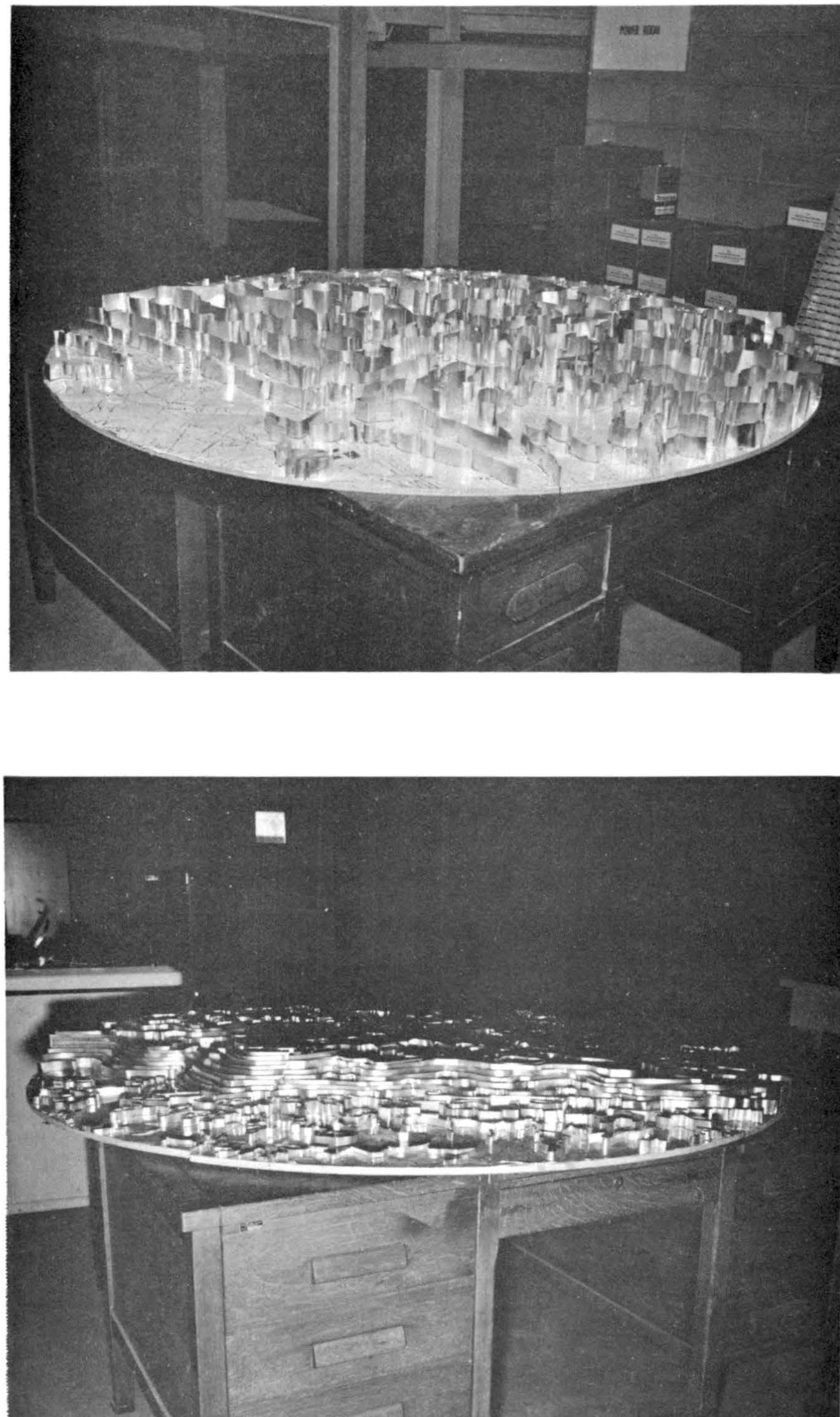

Fig. 8 Model construction, step 1

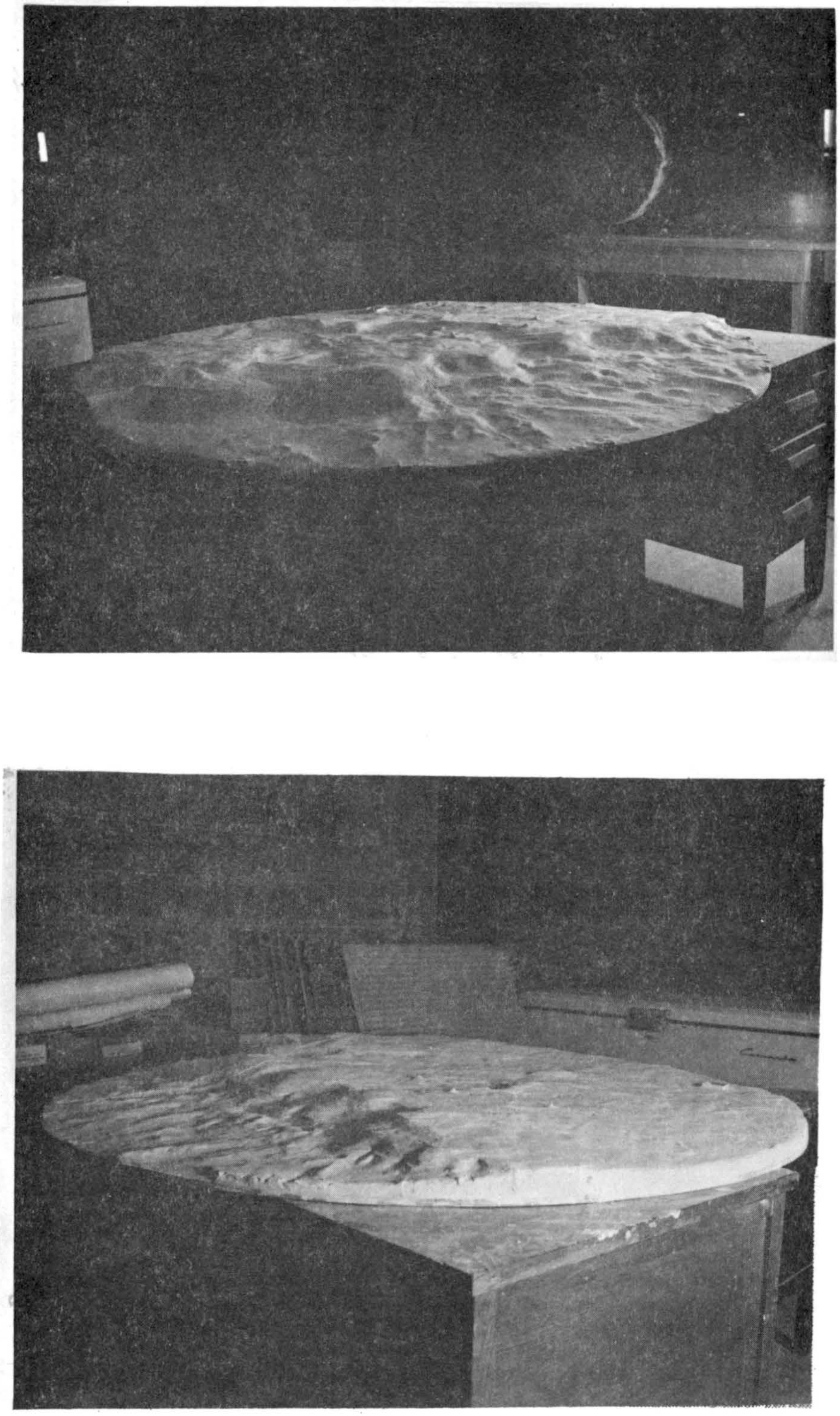

Fig. 9 Model construction, step 2

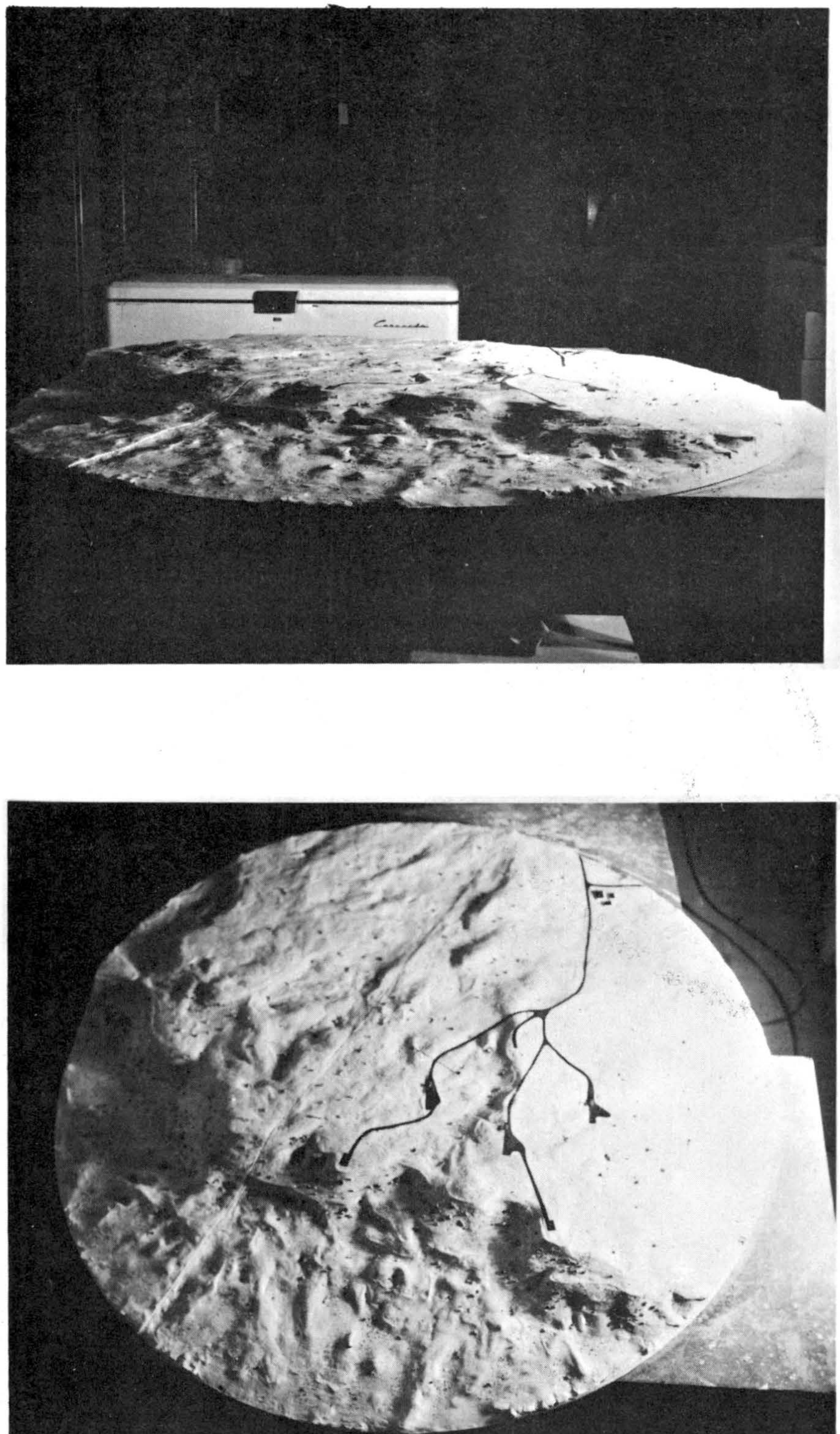

Fig. 10 Model construction, step 3

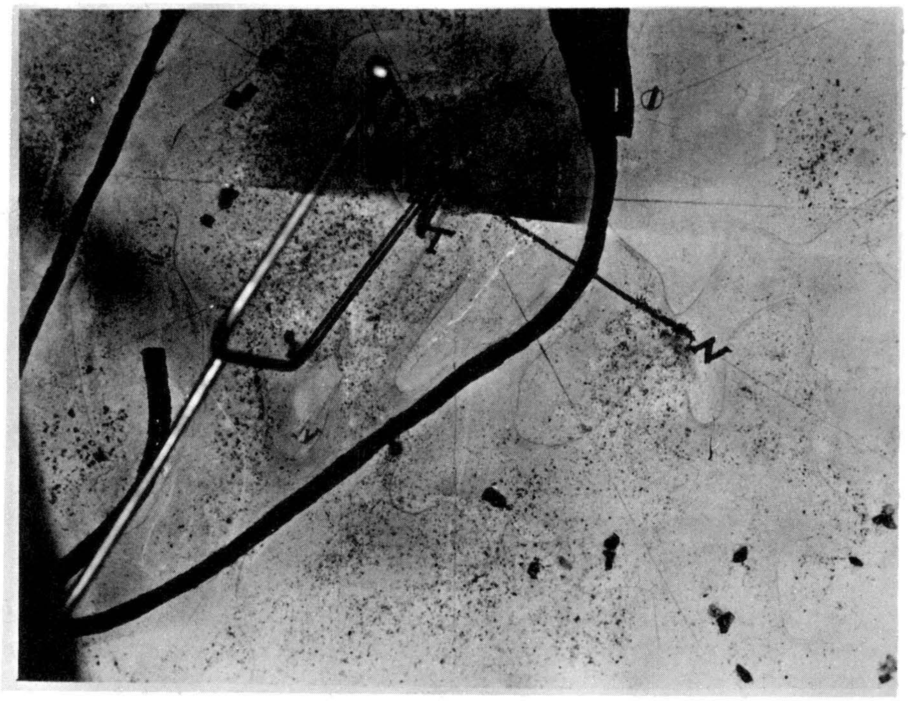

Fig. 11 Tuft method for wind direction measurements

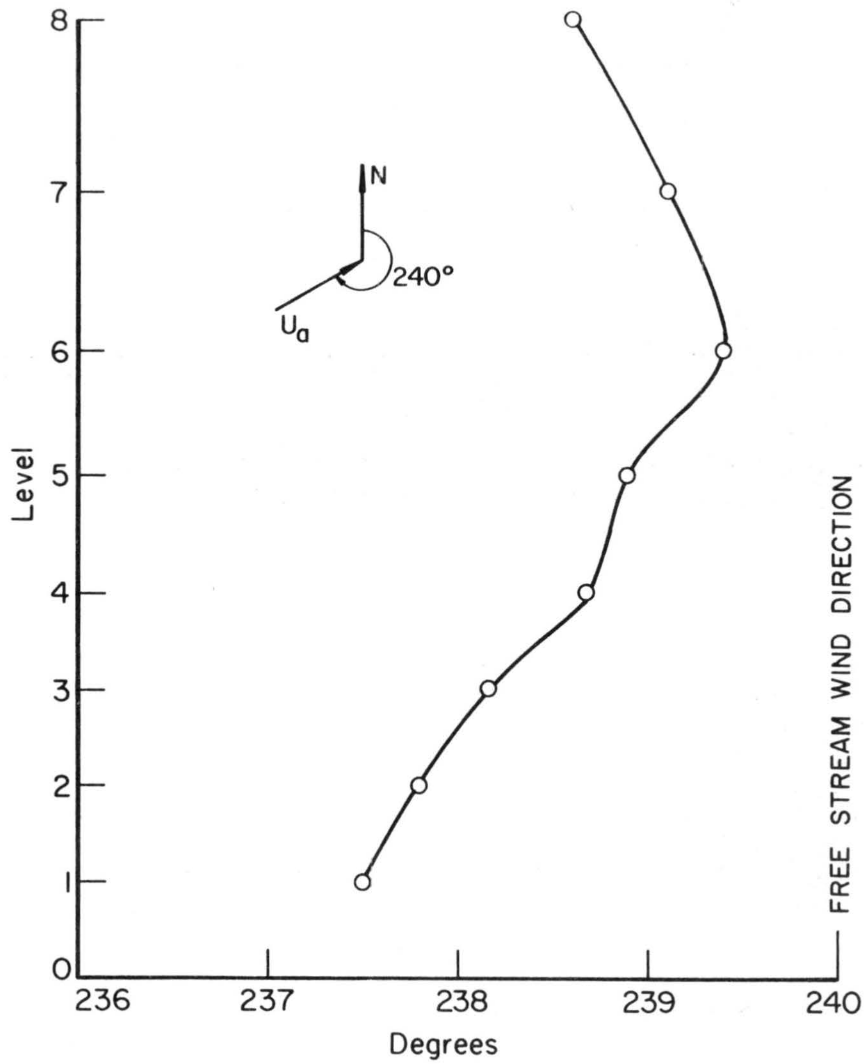

Fig. 12 Wind-vane method for wind direction measurements over model tower site

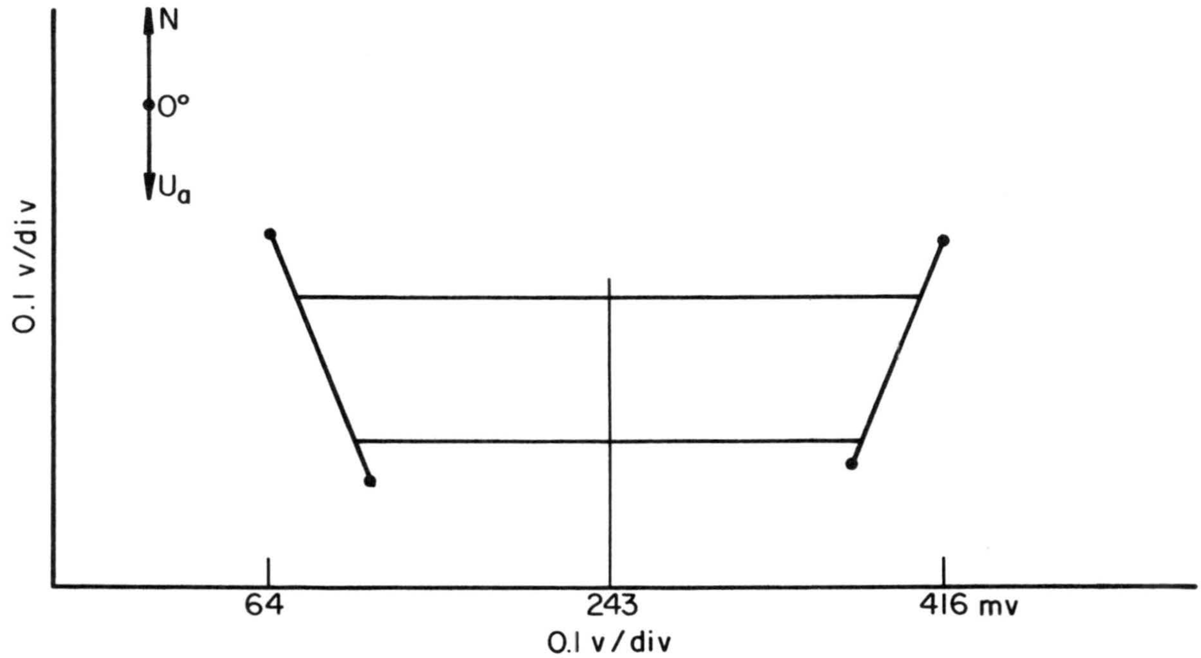

Fig. 13 Wind-direction measurement with hot-wire probe in free stream above tower site

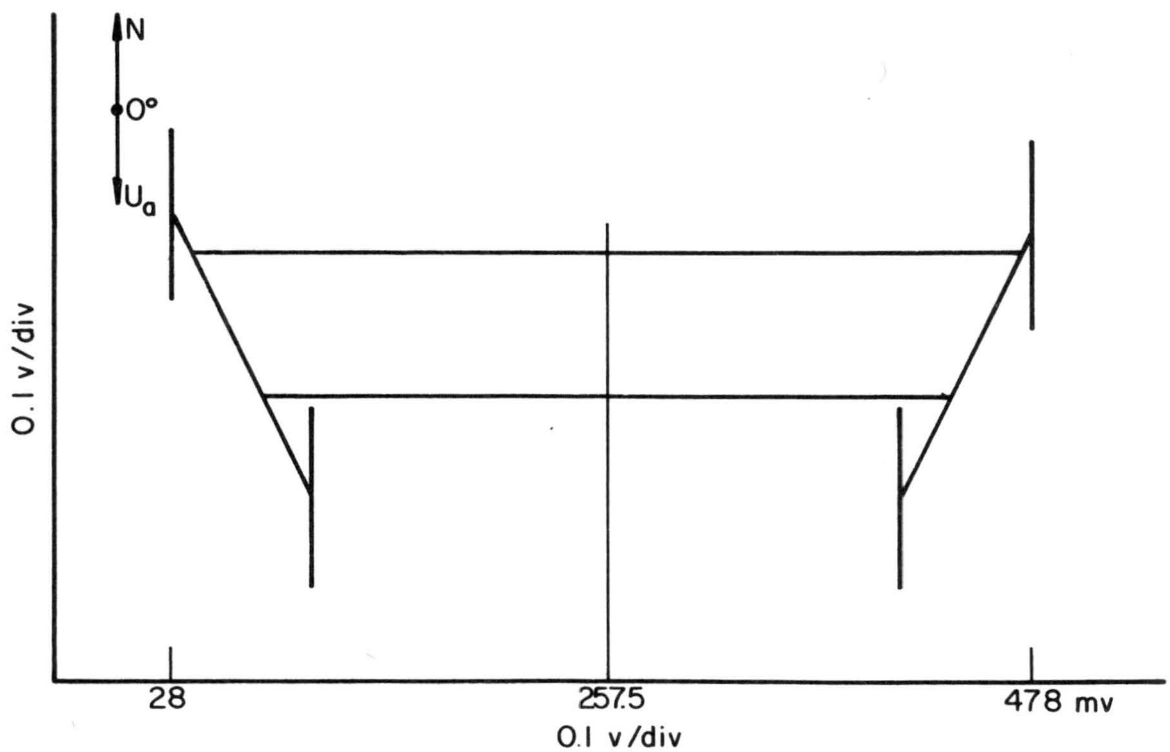

Fig. 14 Wind-direction measurement with hot-wire probe at level one (turbulence region) above tower site

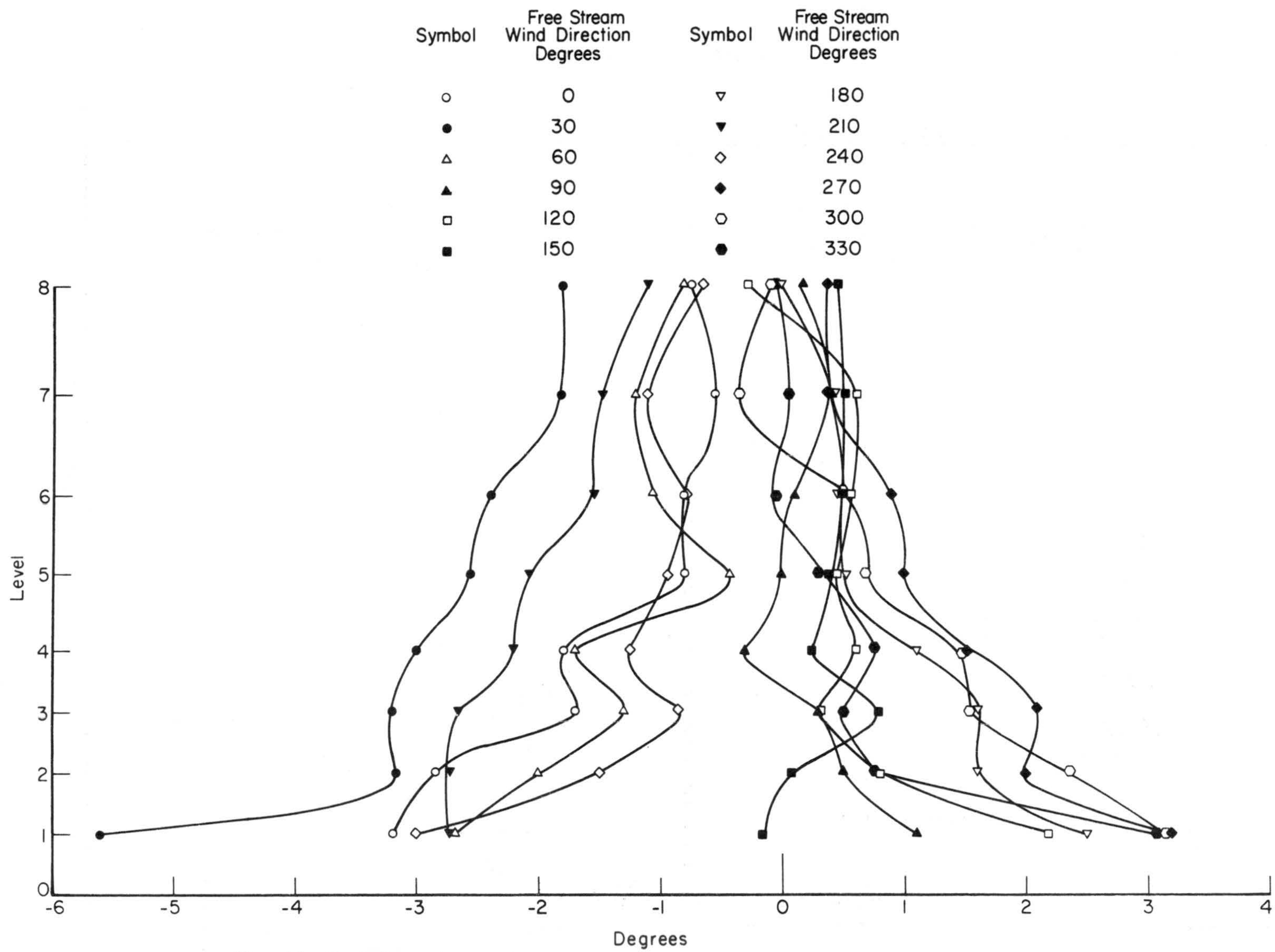

Fig. 15 Wind-direction variation for twelve ambient wind directions over tower site

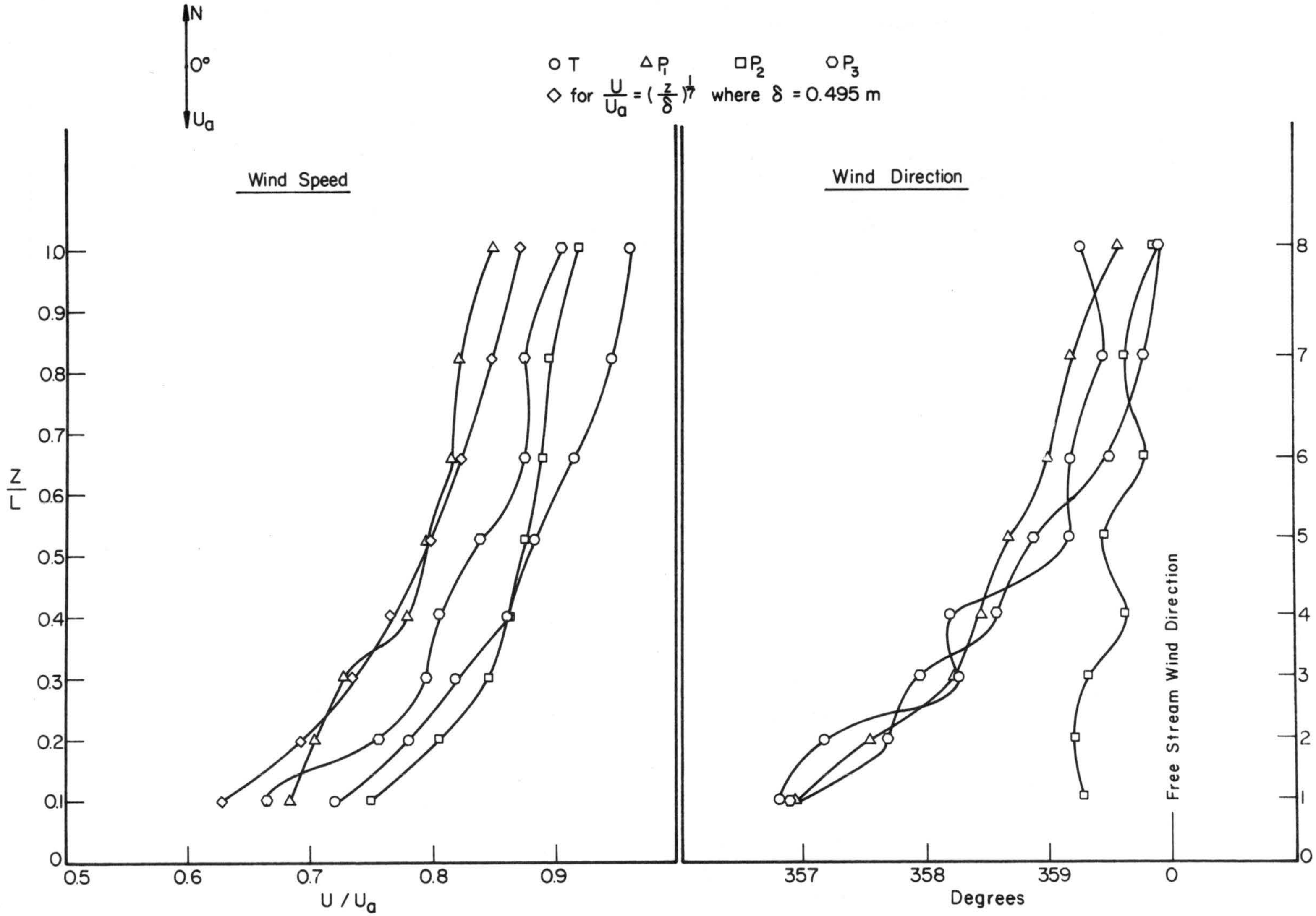

Fig. 16 Wind speed profiles and wind direction profiles at 0 degree free-stream wind direction

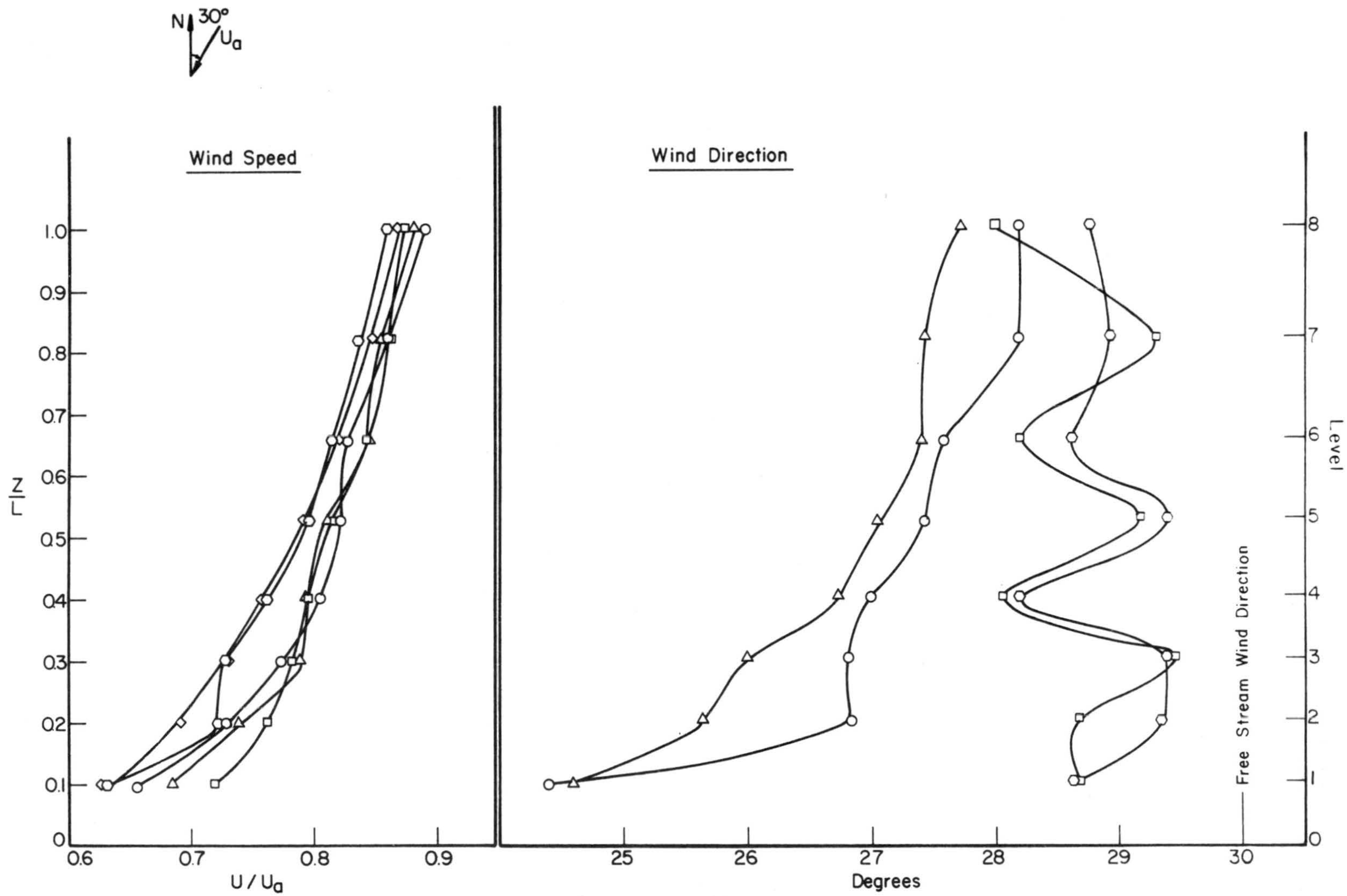

Fig. 17 Wind speed profiles and wind direction profiles at 30 degree free-stream wind direction

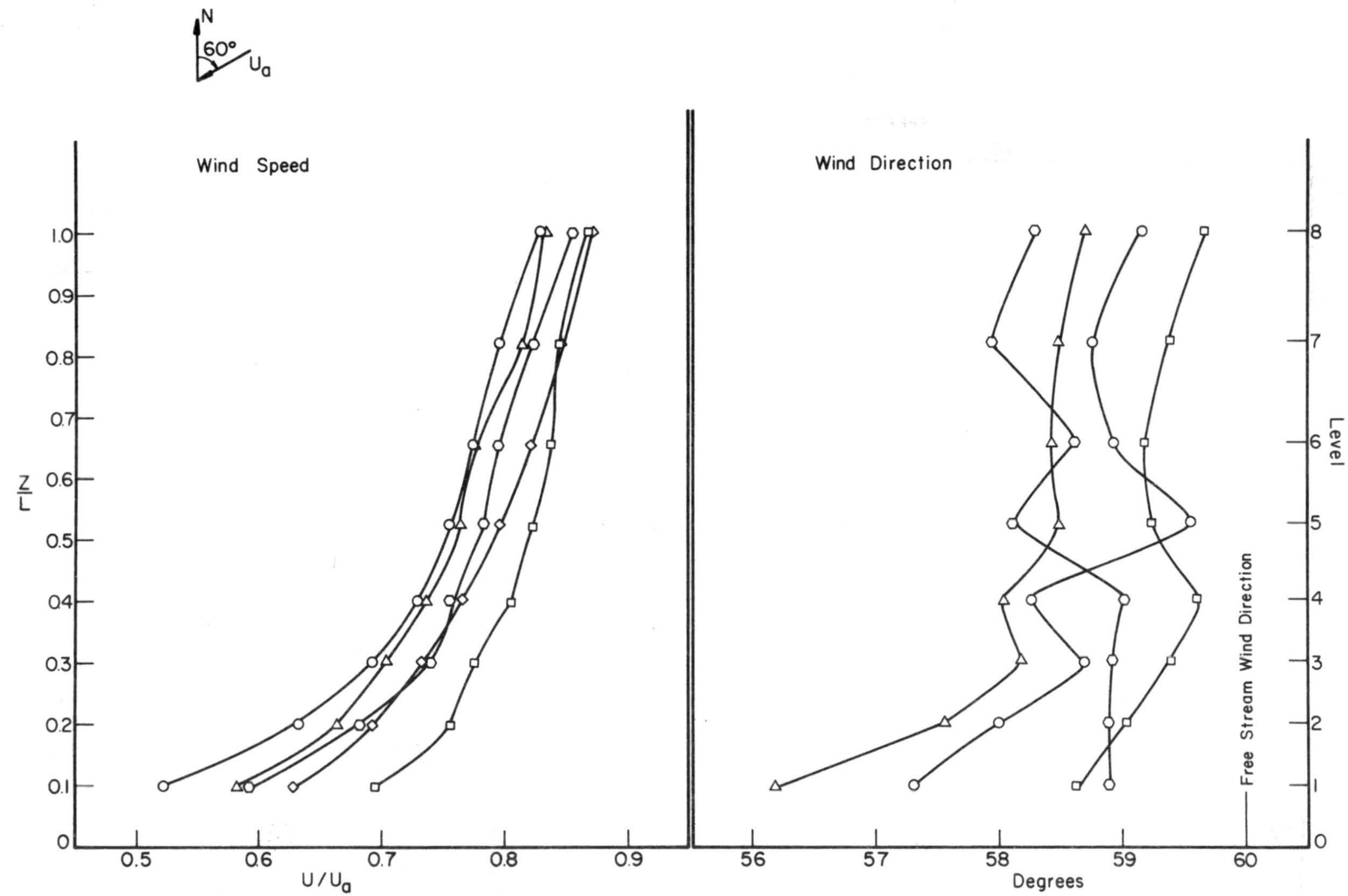

Fig. 18 Wind speed profiles and wind direction profiles at 60 degree free-stream wind direction

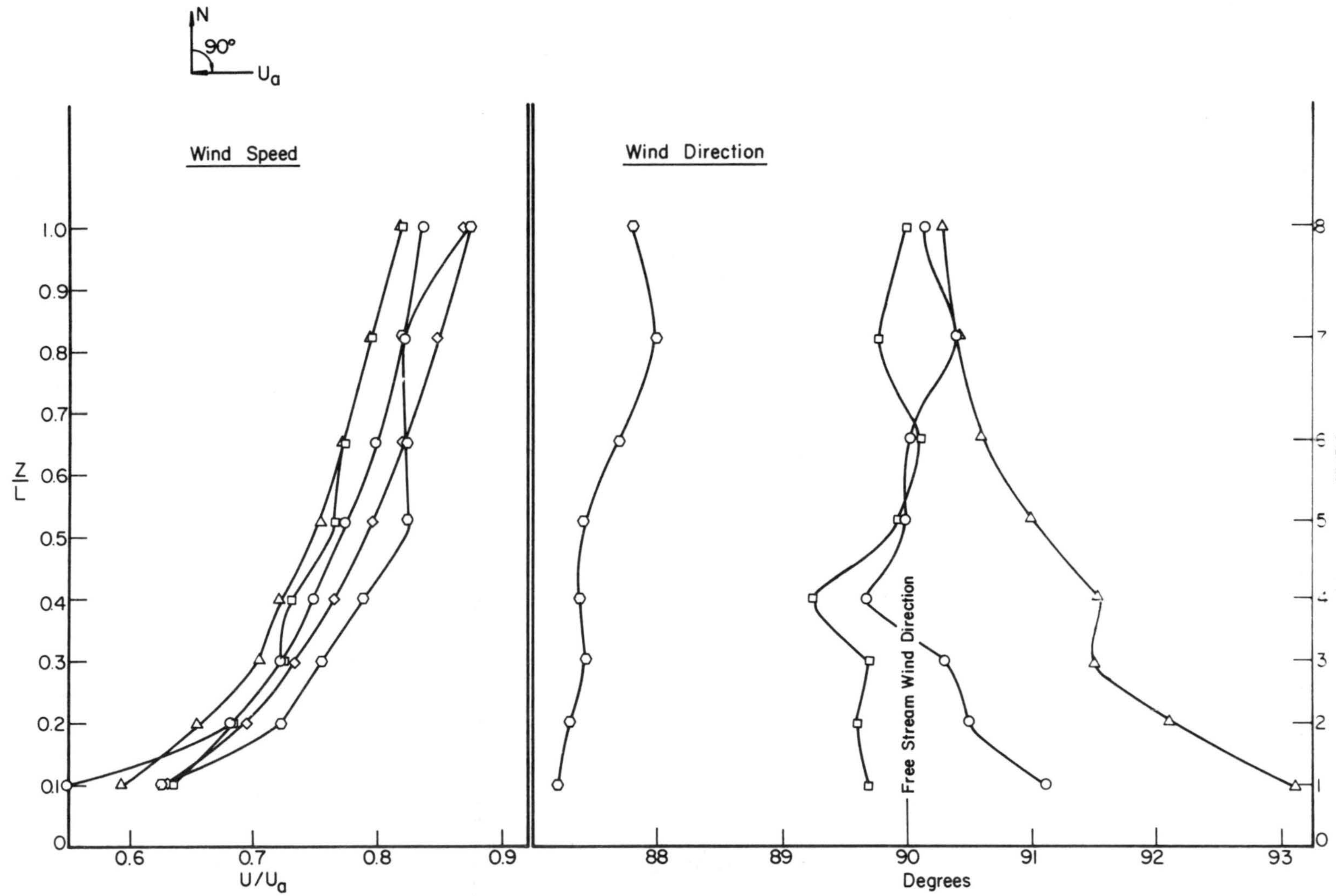

Fig. 19 Wind speed profiles and wind direction profiles at 90 degree free-stream wind direction

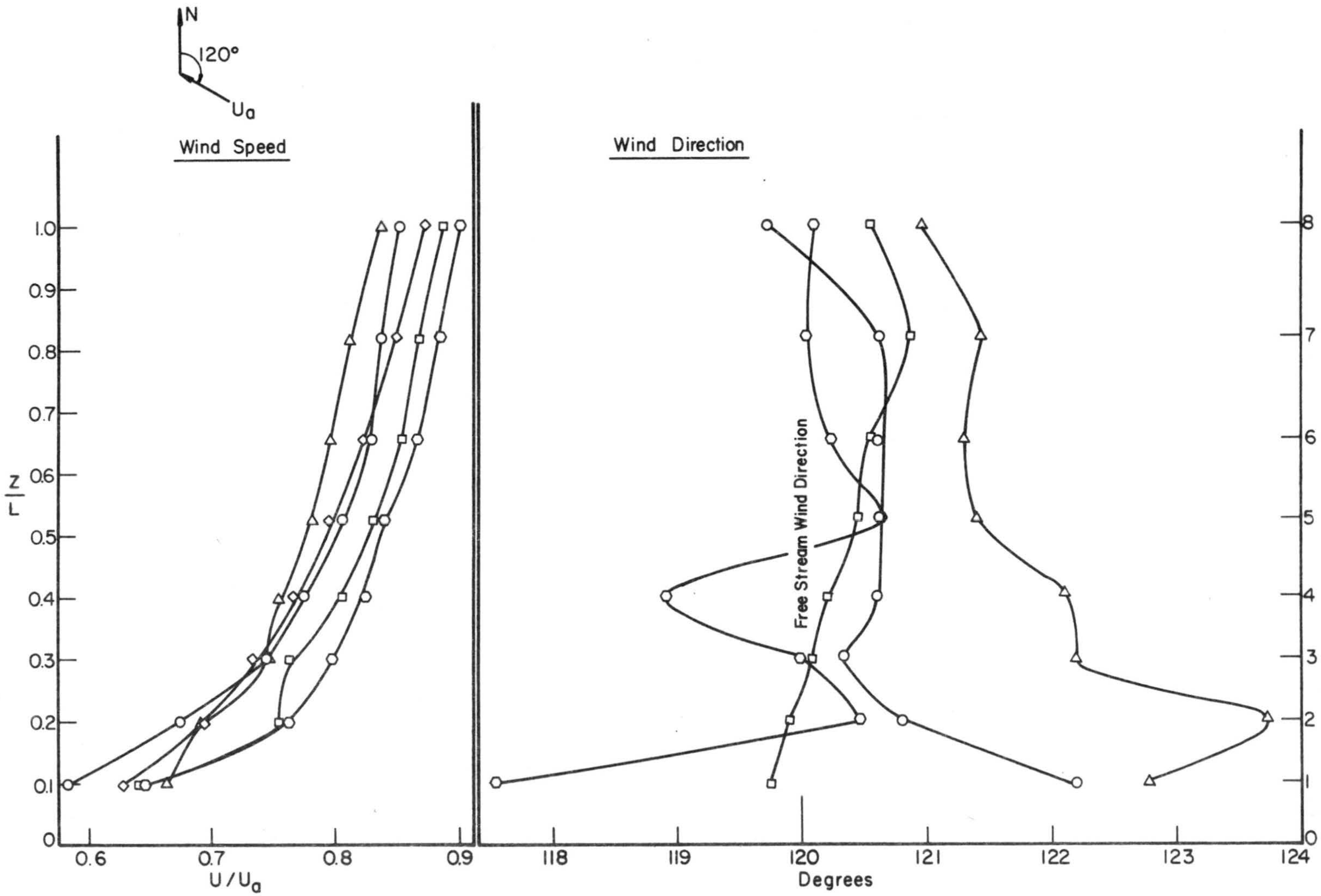

Fig. 20 Wind speed profiles and wind direction profiles at 120 degree free-stream wind direction

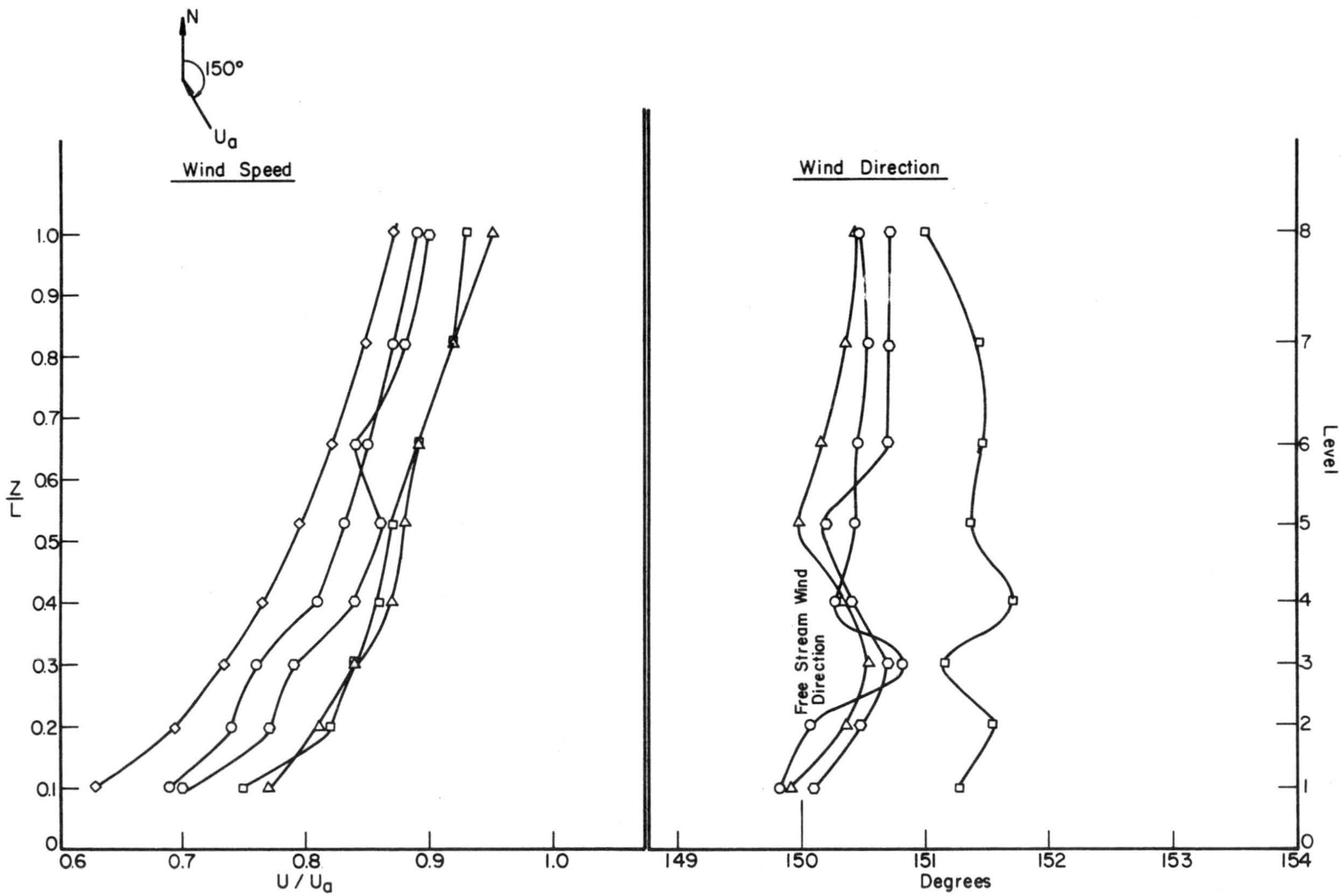

Fig. 21 Wind speed profiles and wind direction profiles at 150 degree free-stream wind direction

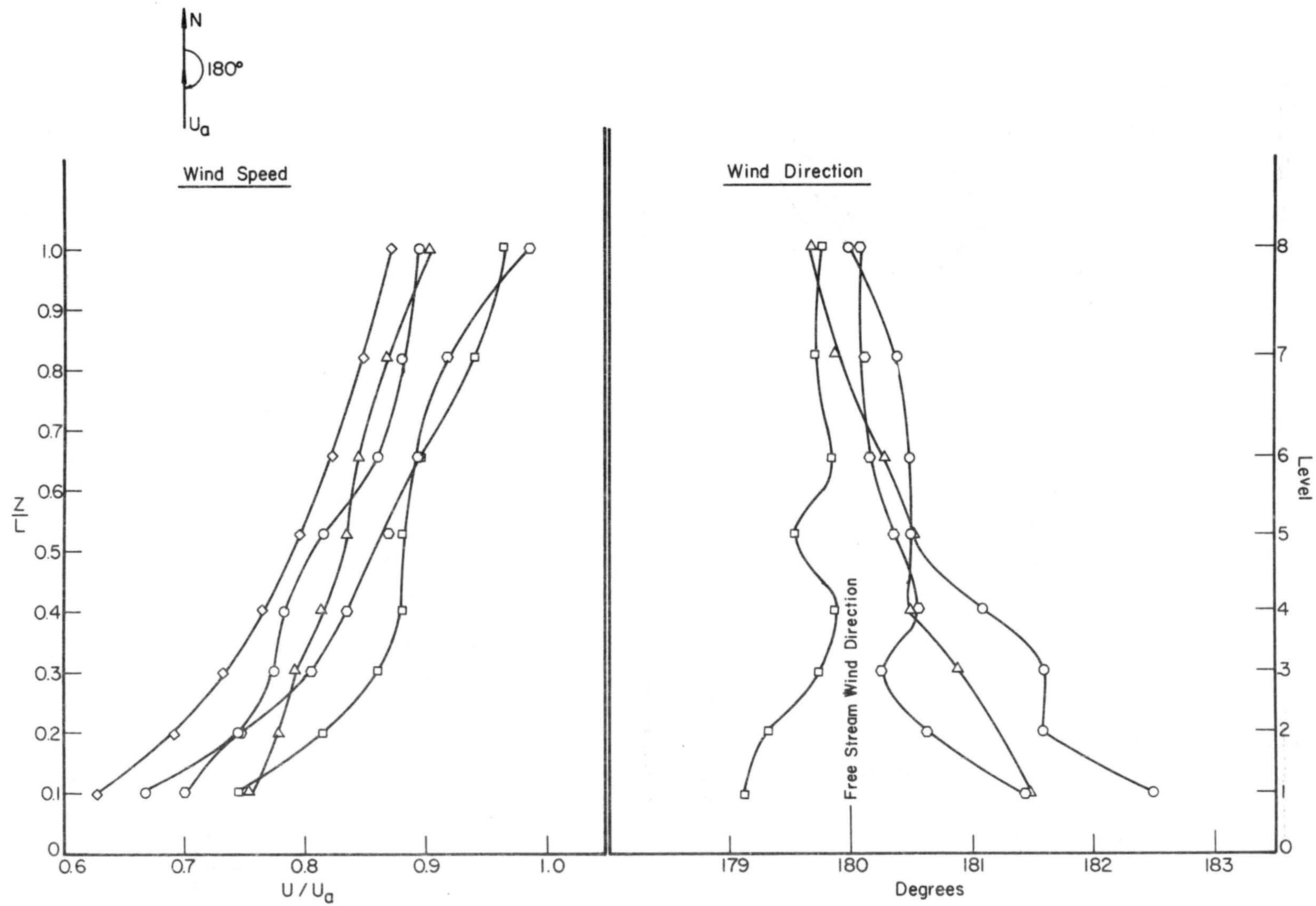

Fig. 22 Wind speed profiles and wind direction profiles at 180 degree free-stream wind direction

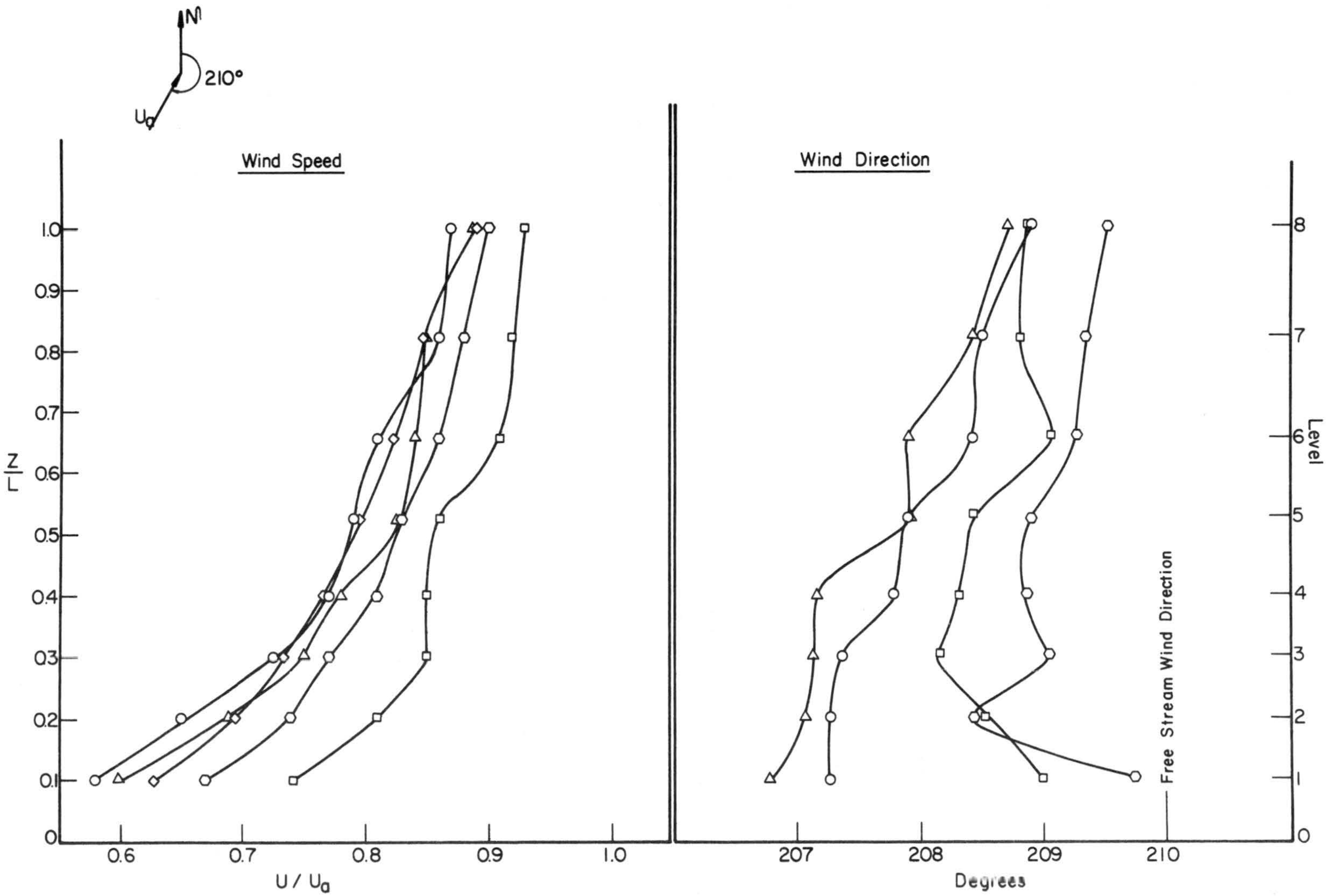

Fig. 23 Wind speed profiles and wind direction profiles at 210 degree free-stream wind direction

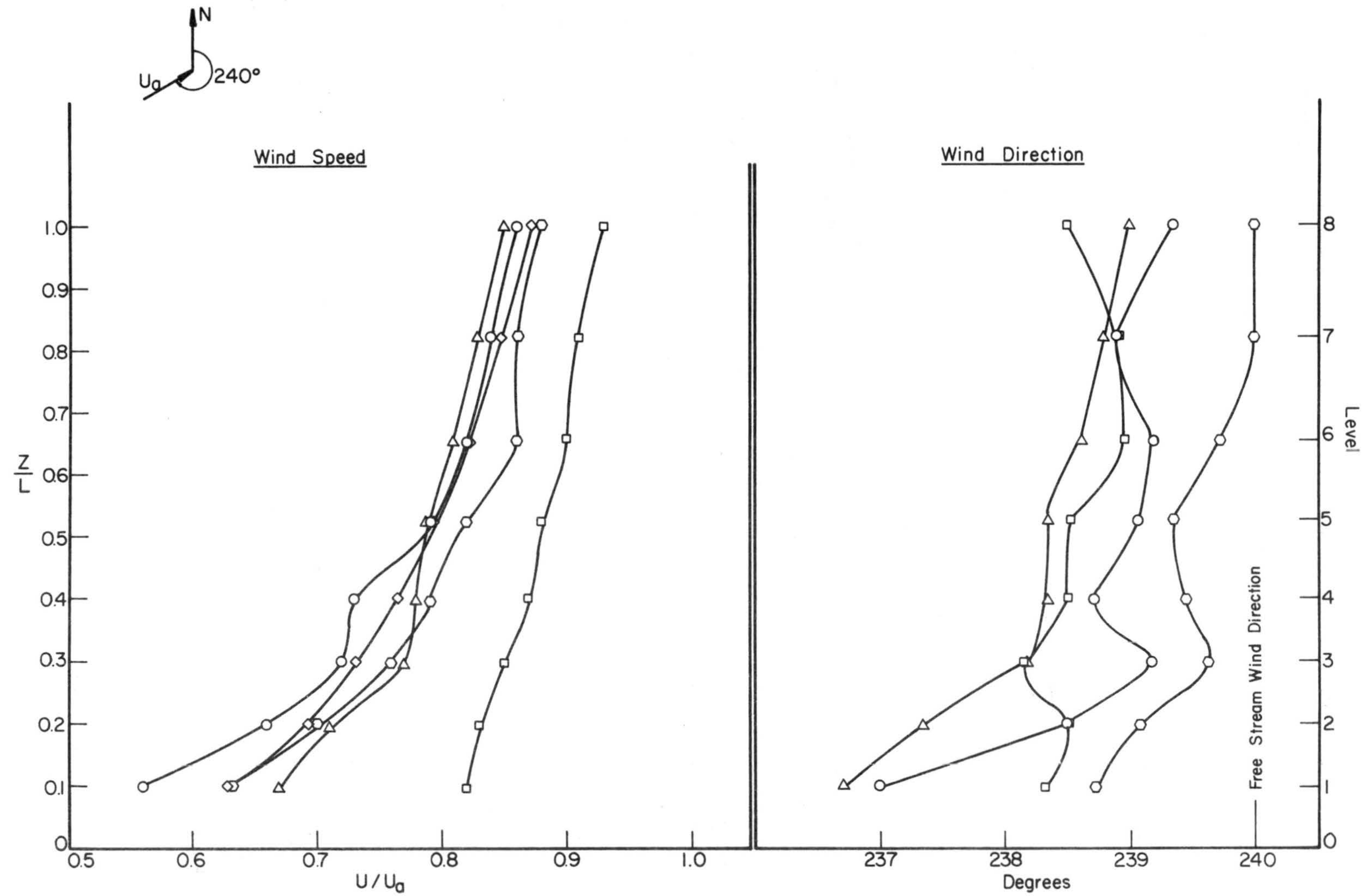

Fig. 24 Wind speed profiles and wind direction profiles at 240 degree free-stream wind direction

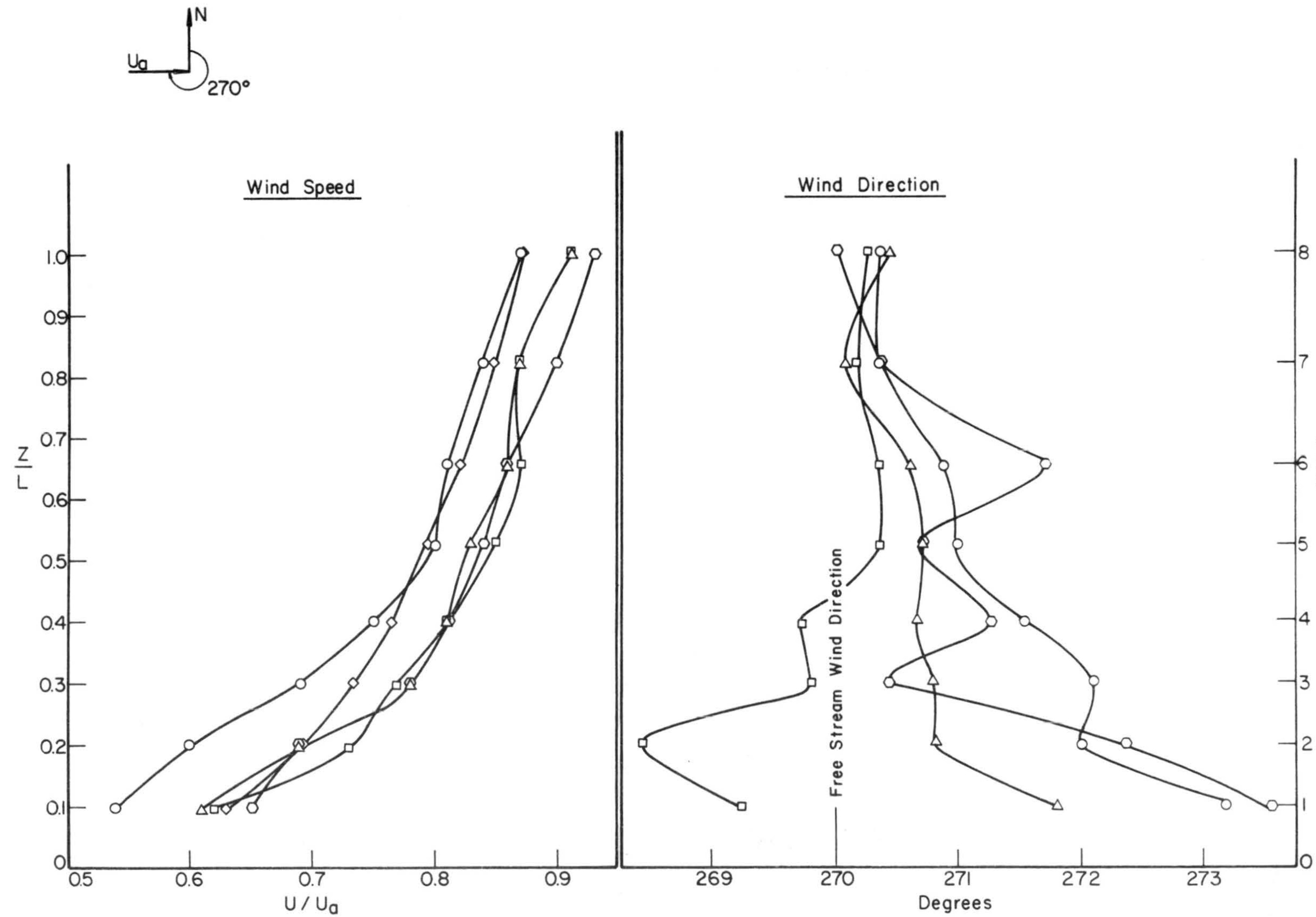

Fig. 25 Wind speed profiles and wind direction profiles at 270 degree free-stream wind direction

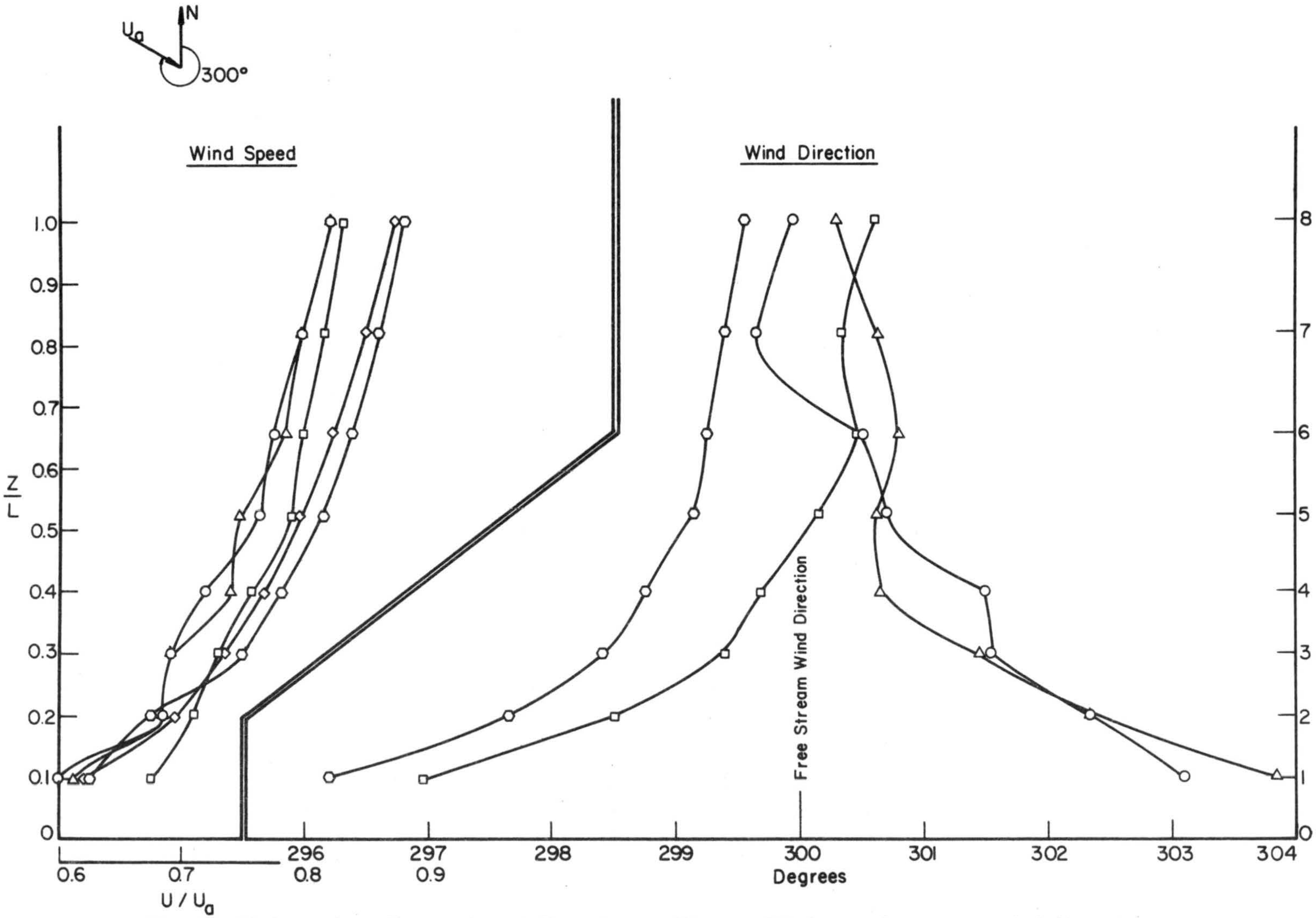

Fig. 26 Wind speed profiles and wind direction profiles at 300 degree free-stream wind direction

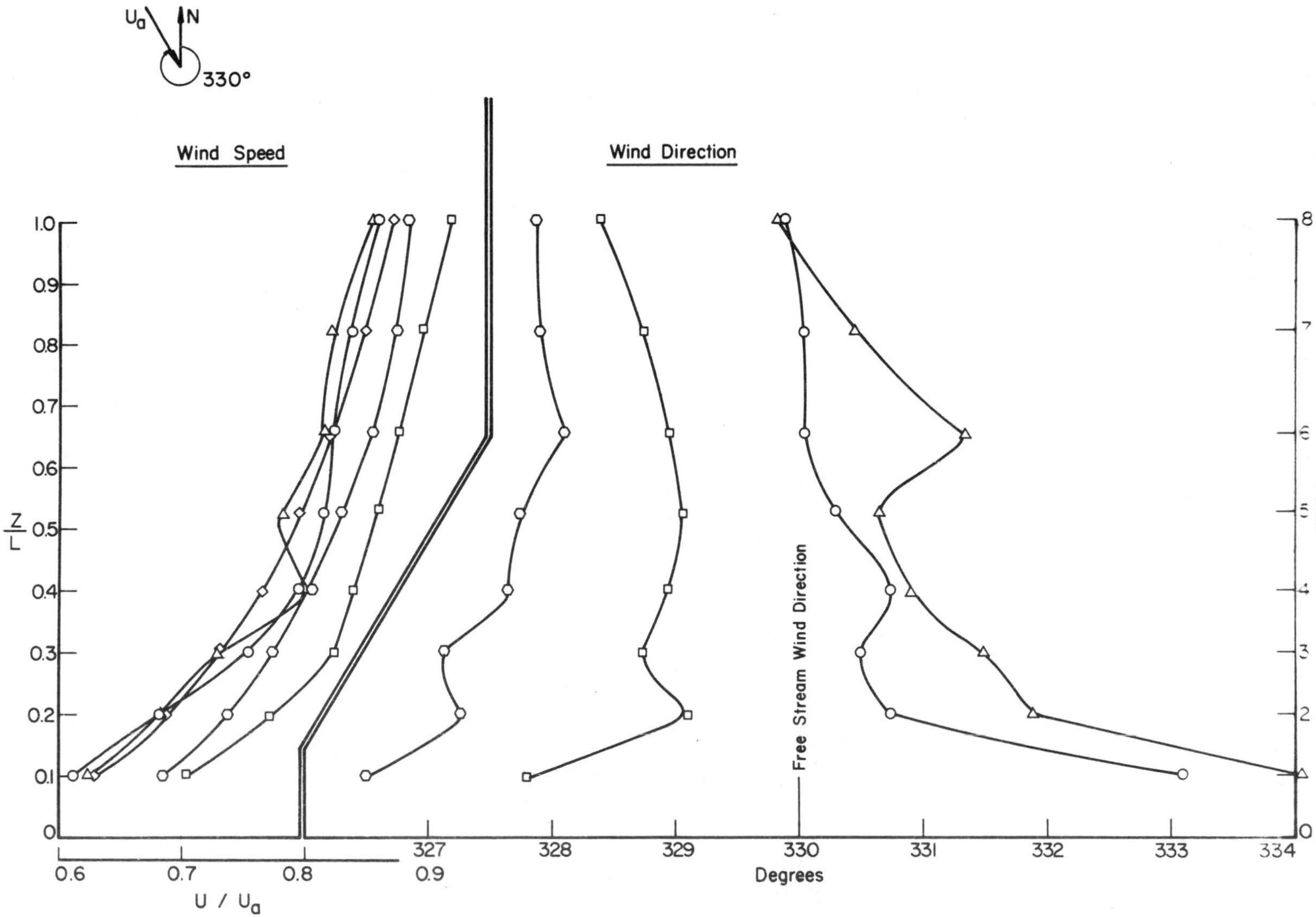

Fig. 27 Wind speed profiles and wind direction profiles at 330 degree free-stream wind direction

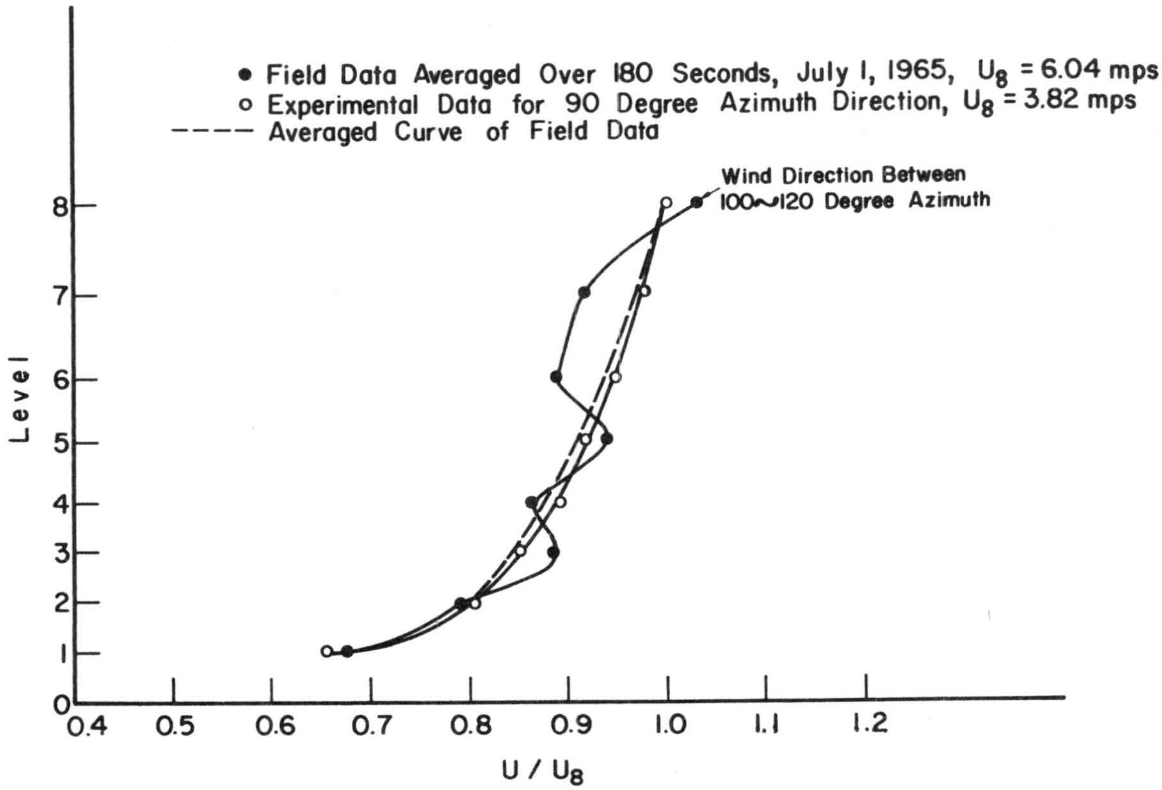

Fig. 28a Mean wind speed profiles over town site in dimensionless form, Green River field data

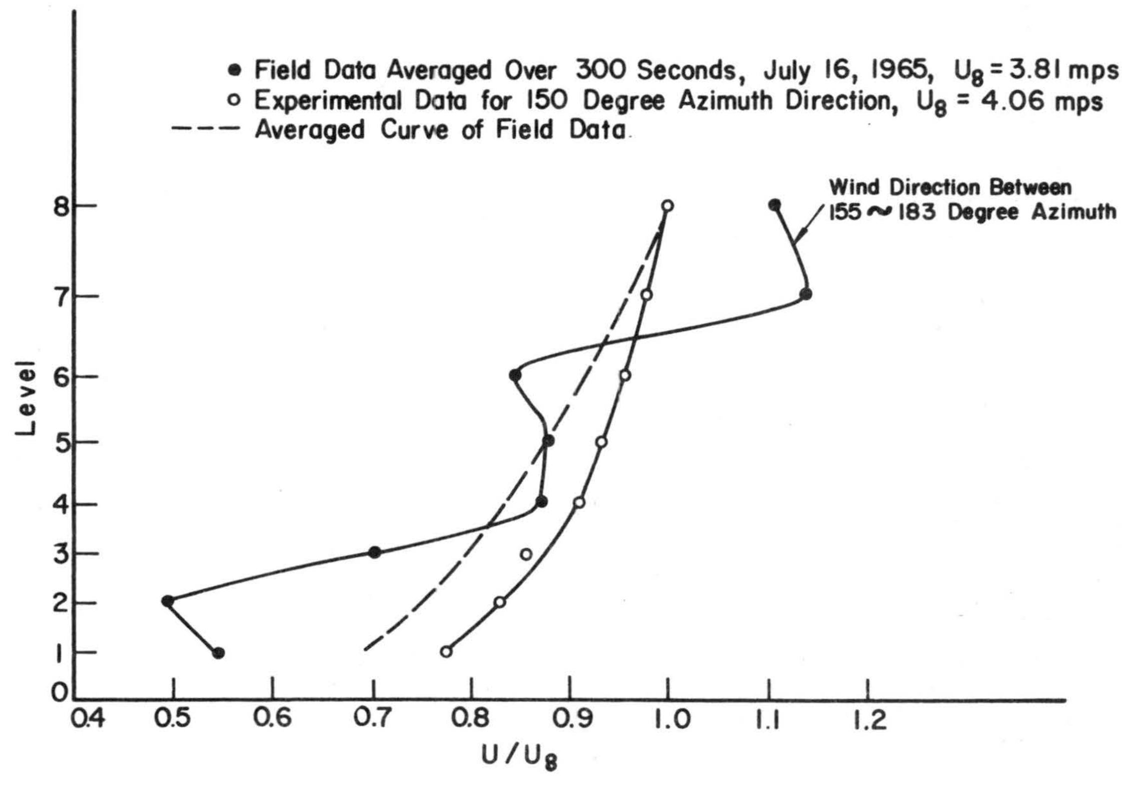

Fig. 28b Mean wind speed profiles over tower site in dimensionless form, Green River field data

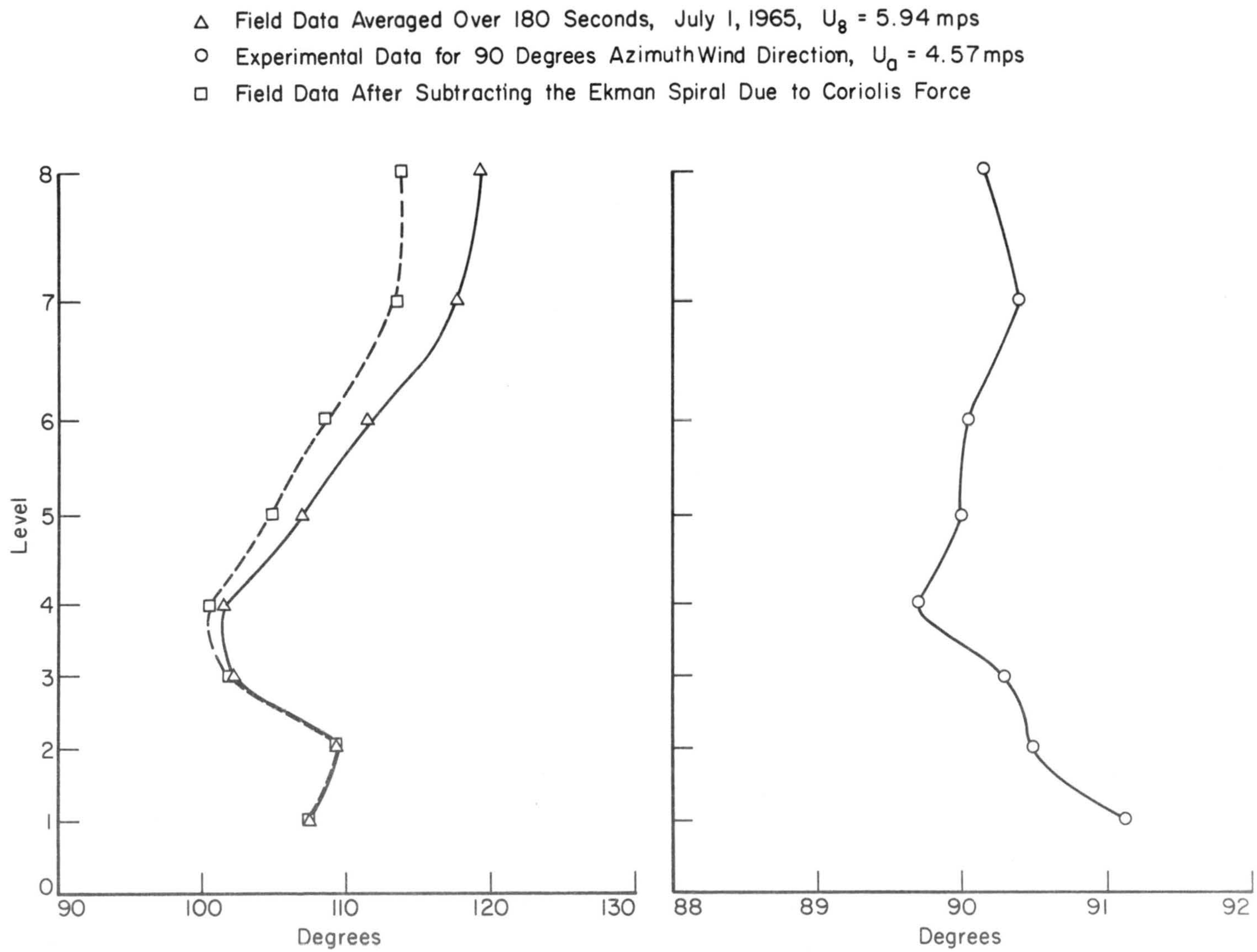

Fig. 29 Mean wind direction variation over tower site, Green River field data

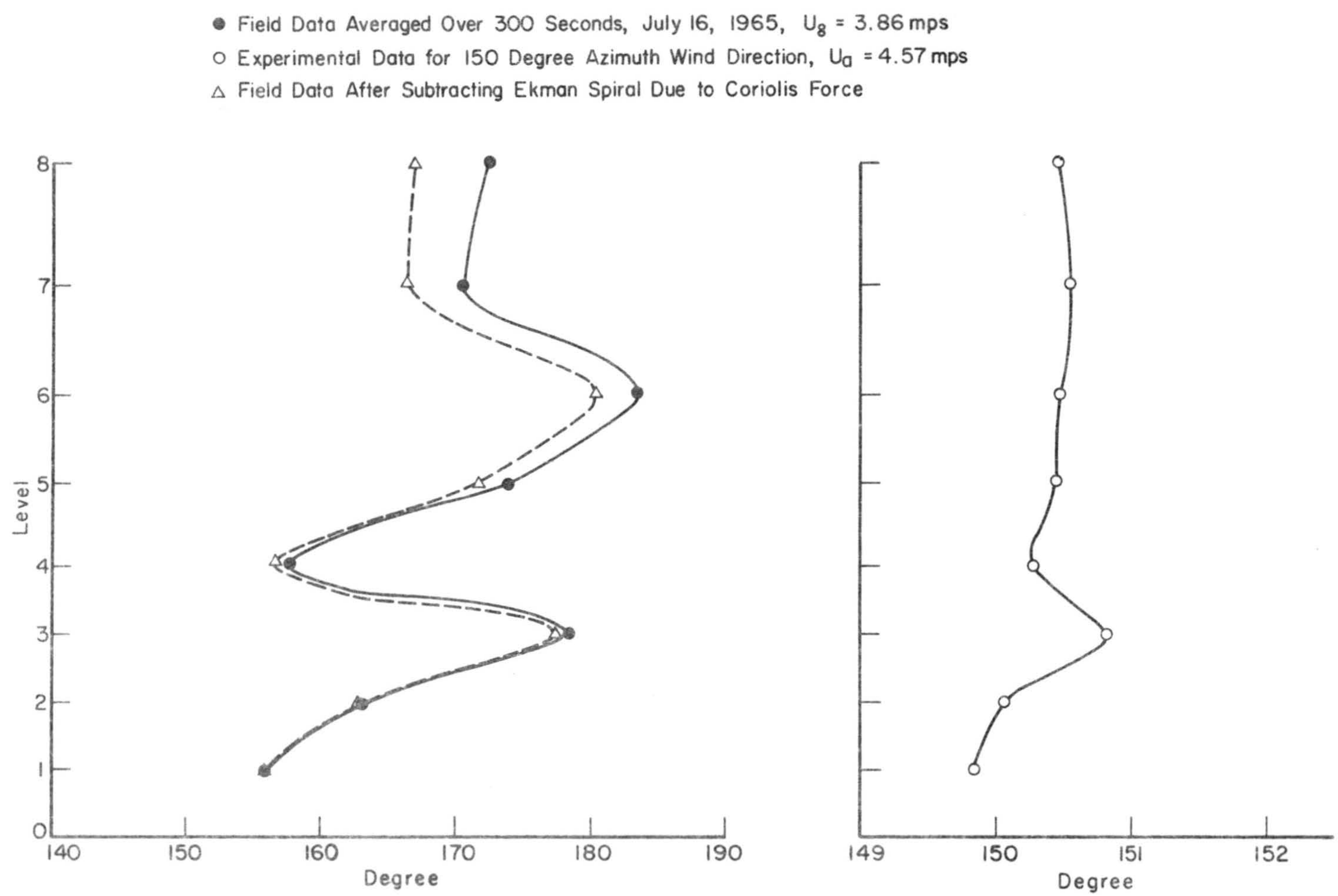

Fig. 29a Mean wind direction variation over tower site, Green River field data

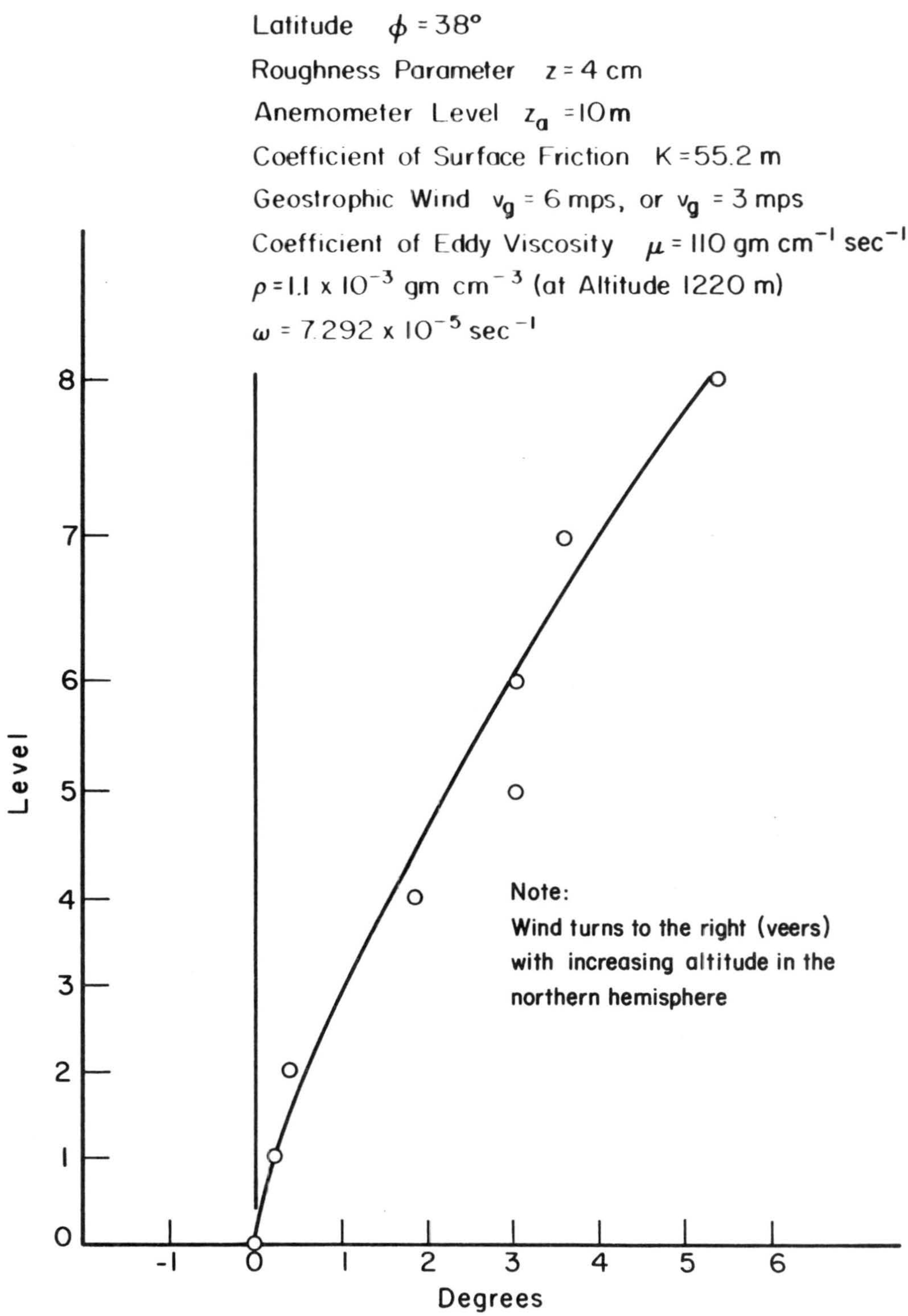

Fig. 29b Wind direction change with altitude, estimated from Ekman Spiral

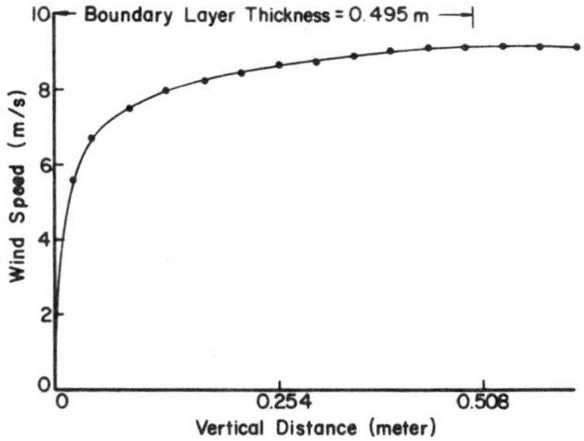

Fig. 30 Boundary-layer profile above the model tower site at 330° free-stream wind direction

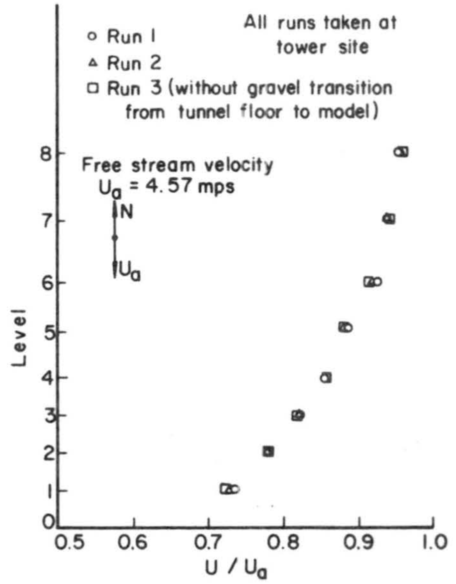

Fig. 31 Reproducibility of mean wind velocity profiles

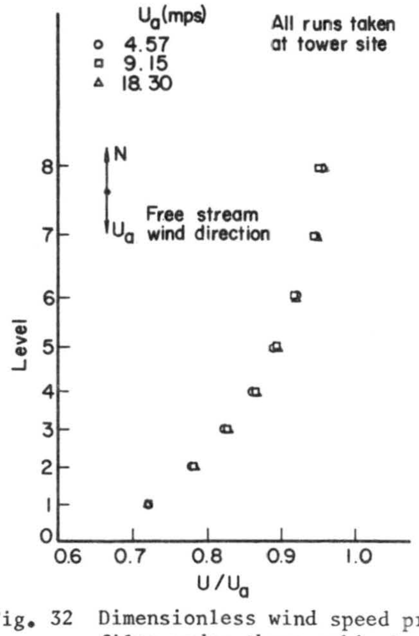

Fig. 32 Dimensionless wind speed profiles under three ambient wind speeds

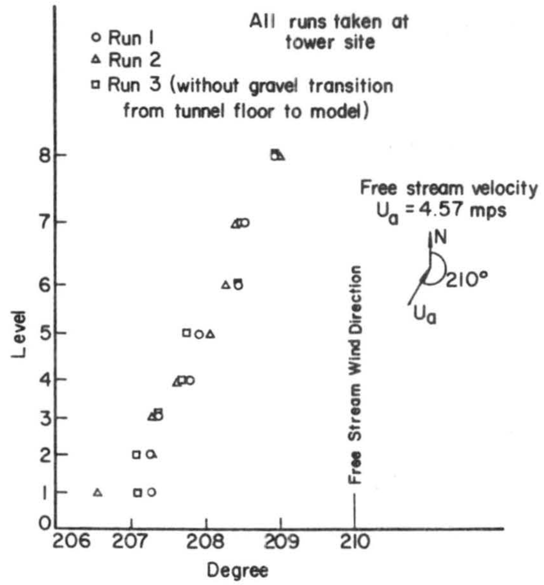

Fig. 33 Reproducibility of wind-direction measurements by hot-wire anemometer

Unclassified
Security Classification

DOCUMENT CONTROL DATA - R&D

(Security classification of title, body of abstract and indexing annotation must be entered when the overall report is classified)

1. ORIGINATING ACTIVITY *(Corporate author)* Colorado State University Foothills Campus Fort Collins, Colorado 80521	2a. REPORT SECURITY CLASSIFICATION Unclassified 2b. GROUP

3. REPORT TITLE

TOPOGRAPHIC INFLUENCES ON WIND NEAR GREEN RIVER, UTAH.

4. DESCRIPTIVE NOTES *(Type of report and inclusive dates)*

Technical Report April 1968

5. AUTHOR(S) *(Last name, first name, initial)*

HSI, G., G. J. BINDER and J. E. CERMAK

6. REPORT DATE	7a. TOTAL NO. OF PAGES	7b. NO. OF REFS
May 1968	50	8

8a. CONTRACT OR GRANT NO. DA-AMC-28-043-65-G20 b. PROJECT NO. 2246 c. d.	9a. ORIGINATOR'S REPORT NUMBER(S) CER67-68GH-GJB-JEC54 9b. OTHER REPORT NO(S) *(Any other numbers that may be assigned this report)*

10. AVAILABILITY/LIMITATION NOTICES

Distribution of this report is unlimited

11. SUPPLEMENTARY NOTES	12. SPONSORING MILITARY ACTIVITY
	U.S. Army Materiel Command Washington, D. C. 20025

13. ABSTRACT

Actual terrain near Green River, Utah, was modeled to a scale of 1:800. The purpose of this study was to find the effect of topography on wind speed and wind direction.

Field data are included in this report and comparisons between model and prototype data are made.

Throughout this study, an ambient wind velocity of 4.57 mps was used and a neutral flow condition was maintained in the Army Meteorological Wind Tunnel.

DD FORM 1 JAN 64 1473

Unclassified
Security Classification

Unclassified

Security Classification

14. KEY WORDS	LINK A		LINK B		LINK C	
	ROLE	WT	ROLE	WT	ROLE	WT
Atmospheric Modeling						
Topographic influence on winds						
Atmospheric surface layer						
Wind variability						
Fluid mechanics						
Wind tunnel simulation						

INSTRUCTIONS

1. ORIGINATING ACTIVITY: Enter the name and address of the contractor, subcontractor, grantee, Department of Defense activity or other organization *(corporate author)* issuing the report.

2*a*. REPORT SECURITY CLASSIFICATION: Enter the overall security classification of the report. Indicate whether "Restricted Data" is included. Marking is to be in accordance with appropriate security regulations.

2*b*. GROUP: Automatic downgrading is specified in DoD Directive 5200.10 and Armed Forces Industrial Manual. Enter the group number. Also, when applicable, show that optional markings have been used for Group 3 and Group 4 as authorized.

3. REPORT TITLE: Enter the complete report title in all capital letters. Titles in all cases should be unclassified. If a meaningful title cannot be selected without classification, show title classification in all capitals in parenthesis immediately following the title.

4. DESCRIPTIVE NOTES: If appropriate, enter the type of report, e.g., interim, progress, summary, annual, or final. Give the inclusive dates when a specific reporting period is covered.

5. AUTHOR(S): Enter the name(s) of author(s) as shown on or in the report. Enter last name, first name, middle initial. If military, show rank and branch of service. The name of the principal author is an absolute minimum requirement.

6. REPORT DATE: Enter the date of the report as day, month, year; or month, year. If more than one date appears on the report, use date of publication.

7*a*. TOTAL NUMBER OF PAGES: The total page count should follow normal pagination procedures, i.e., enter the number of pages containing information.

7*b*. NUMBER OF REFERENCES: Enter the total number of references cited in the report.

8*a*. CONTRACT OR GRANT NUMBER: If appropriate, enter the applicable number of the contract or grant under which the report was written.

8*b*, 8*c*, & 8*d*. PROJECT NUMBER: Enter the appropriate military department identification, such as project number, subproject number, system numbers, task number, etc.

9*a*. ORIGINATOR'S REPORT NUMBER(S): Enter the official report number by which the document will be identified and controlled by the originating activity. This number must be unique to this report.

9*b*. OTHER REPORT NUMBER(S): If the report has been assigned any other report numbers *(either by the originator or by the sponsor)*, also enter this number(s).

10. AVAILABILITY/LIMITATION NOTICES: Enter any limitations on further dissemination of the report, other than those imposed by security classification, using standard statements such as:

(1) "Qualified requesters may obtain copies of this report from DDC."

(2) "Foreign announcement and dissemination of this report by DDC is not authorized."

(3) "U. S. Government agencies may obtain copies of this report directly from DDC. Other qualified DDC users shall request through

_______________."

(4) "U. S. military agencies may obtain copies of this report directly from DDC. Other qualified users shall request through

_______________."

(5) "All distribution of this report is controlled. Qualified DDC users shall request through

_______________."

If the report has been furnished to the Office of Technical Services, Department of Commerce, for sale to the public, indicate this fact and enter the price, if known.

11. SUPPLEMENTARY NOTES: Use for additional explanatory notes.

12. SPONSORING MILITARY ACTIVITY: Enter the name of the departmental project office or laboratory sponsoring *(paying for)* the research and development. Include address.

13. ABSTRACT: Enter an abstract giving a brief and factual summary of the document indicative of the report, even though it may also appear elsewhere in the body of the technical report. If additional space is required, a continuation sheet shall be attached.

It is highly desirable that the abstract of classified reports be unclassified. Each paragraph of the abstract shall end with an indication of the military security classification of the information in the paragraph, represented as *(TS)*, *(S)*, *(C)*, or *(U)*.

There is no limitation on the length of the abstract. However, the suggested length is from 150 to 225 words.

14. KEY WORDS: Key words are technically meaningful terms or short phrases that characterize a report and may be used as index entries for cataloging the report. Key words must be selected so that no security classification is required. Identifiers, such as equipment model designation, trade name, military project code name, geographic location, may be used as key words but will be followed by an indication of technical context. The assignment of links, rules, and weights is optional.

Unclassified

Security Classification

MINIMUM BASIC DISTRIBUTION LIST FOR USAMC SCIENTIFIC AND TECHNICAL REPORTS IN METEOROLOGY AND ATMOSPHERIC SCIENCES

Commanding General (1)
U. S. Army Materiel Command
Attn: AMCRD-RV-A
Washington, D. C. 20315

Commanding General (1)
U. S. Army Electronics Command
Attn: AMSEL-EW
Fort Monmouth, New Jersey 07703

Commanding General (1)
U. S. Army Test and Evaluation Command
Attn: NBC Directorate
Aberdeen Proving Ground, Maryland 21005

Commanding Officer (1)
U. S. Army Ballistics Research Laboratories
Attn: AMXBR-IA
Aberdeen Proving Ground, Maryland 21005

Chief, Atmospheric Physics Division (2)
Atmospheric Sciences Laboratory
U. S. Army Electronics Command
Fort Monmouth, New Jersey 07703

U. S. Army Munitions Command (1)
Attn: Irving Solomon
Operations Research Group
Edgewood Arsenal, Maryland 21010

Commanding Officer (1)
U. S. Army Dugway Proving Ground
Attn: Meteorology Division
Dugway, Utah 84022

Commanding Officer (1)
U. S. Army CDC, CBR Agency
Attn: Mr. N. W. Bush
Fort McClellan, Alabama 36205

Commanding General (1)
U. S. Army Test and Evaluation Command
Attn: AMSTE-EL
Aberdeen Proving Ground, Maryland 21005

Commandant (1)
U. S. Army Signal School
Attn: Meteorological Department
Fort Monmouth, New Jersey 07703

Assistant Chief of Staff for Force Development (1)
CBR Nuclear Operations Directorate
Department of the Army
Washington, D. C. 20310

Director (1)
Atmospheric Sciences Programs
National Sciences Foundation
Washington, D. C. 20550

Assistant Secretary of Defense (1)
Research and Engineering
Attn: Technical Library
Washington, D. C. 20301

R. A. Taft Sanitary Engineering Center (1)
Public Health Service
4676 Columbia Parkway
Cincinnati, Ohio

Dr. Hans A. Panofsky (1)
Department of Meteorology
The Pennsylvania State University
University Park, Pennsylvania

Commanding General (1)
U. S. Continental Army Command
Attn: Reconnaissance Branch ODCS for Intelligence
Fort Monroe, Virginia 23351

Commander (1)
Air Force Cambridge Research Laboratories
Attn: CRZW
1065 Main Street
Waltham, Massachusetts

President (1)
U. S. Army Artillery Board
Fort Sill, Oklahoma 73504

National Center for Atmospheric Research (1)
Attn: Library
Boulder, Colorado

Dr. J. E. Cermak, Head (15)
Fluid Mechanics Program
Colorado State University
Fort Collins, Colorado 80521

Author (1)

Chief of Research and Development (1)
Department of the Army
Attn: CRD/M
Washington, D. C. 20310

Commanding General (1)
U. S. Army Missile Command
Attn: AMSMI-RRA
Redstone Arsenal, Alabama 35809

Commanding General (1)
U. S. Army Natick Laboratories
Attn: Earth Sciences Division
Natick, Massachusetts 01762

Director, U. S. Army Engineer (1)
Waterways Experiment Station
Attn: WES-FV
Vicksburg, Mississippi 39181

Chief, Atmospheric Sciences Research Division (5)
Atmospheric Sciences Laboratory
U. S. Army Electronics Command
Fort Huachuca, Arizona 85613

Commanding Officer (1)
U. S. Army Frankford Arsenal
Attn: SMUFA-1140
Philadelphia, Pennsylvania 19137

Commandant (1)
U. S. Army Artillery and Missile School
Attn: Target Acquisition Department
Fort Sill, Oklahoma 73504

Commanding General (1)
U. S. Army Electronics Proving Ground
Attn: Field Test Department
Fort Huachuca, Arizona 85613

Commanding General (1)
U. S. Army Test and Evaluation Command
Attn: AMSTE-BAF
Aberdeen Proving Ground, Maryland 21005

Office of Chief Communications - Electronics (1)
Department of the Army
Attn: Electronics Systems Directorate
Washington, D. C. 20315

Chief of Naval Operations (1)
Department of the Navy
Attn: Code 427
Washington, D. C. 20350

Director (1)
Bureau of Research and Development
Federal Aviation Agency
Washington, D. C. 20553

Director of Meteorological Systems (1)
Office of Applications (FM)
National Aeronautics and Space Administration
Washington, D. C. 20546

Director (1)
Atmospheric Physics and Chemistry Laboratory
Environmental Science Services Administration
Boulder, Colorado

Andrew Morse (1)
Army Aeronautical Activity
Ames Research Center
Moffett Field, California 94035

Commanding Officer (2)
U. S. Army Cold Regions Research and Engineering Laboratories
Attn: Environmental Research Branch
Hanover, New Hampshire 03755

Mr. Ned L. Kragness (1)
U. S. Army Aviation Materiel Command
SMOSM-E
12th and Spruce Streets
Saint Louis, Missouri 63166

Commanding Officer, U. S. Army (1)
Artillery Combat Development Agency
Fort Sill, Oklahoma 73504

Commander, USAR Air Weather Service (MATS) (1)
Attn: AWSSS/TIPD
Scott Air Force Base, Illinois

Dr. John Bogusky (1)
7310 Cedardale Drive
Alexandria, Virginia 22308

Commanding General (1)
U. S. Army Combat Development Command
Attn: CDCMR-E
Fort Belvoir, Virginia 22060

Commanding General (1)
U. S. Army Munitions Command
Attn: AMSMU-RE-R
Dover, New Jersey 07801

Commanding Officer (1)
U. S. Army Ballistics Research Laboratories
Attn: AMXBR-B
Aberdeen Proving Ground, Maryland 21005

Director (2)
Atmospheric Sciences Laboratory
U. S. Army Electronics Command
Fort Monmouth, New Jersey 07703

Chief, Atmospheric Sciences Office (2)
Atmospheric Sciences Laboratory
U. S. Army Electronics Command
White Sands Missile Range, New Mexico 88002

Commanding Officer (1)
U. S. Army Picatinny Arsenal
Attn: SMUPA-TV-3
Dover, New Jersey 07801

Commanding Officer (1)
U. S. Army Communications - Electronics Combat Development Agency
Fort Monmouth, New Jersey 07703

Commanding General (1)
Deseret Test Center
Attn: Design and Analysis Division
Fort Douglas, Utah 84113

Commandant (1)
U. S. Army CBR School Micrometeorological Section
Fort McClellan, Alabama 36205

Assistant Chief of Staff for Intelligence (1)
Department of the Army
Attn: ACSI-DERSI
Washington, D. C. 20310

Officer in Charge (1)
U. S. Naval Weather Research Facility
U. S. Naval Air Station, Building 4-28
Norfolk, Virginia 23500

Chief, Fallout Studies Branch (1)
Division of Biology and Medicine
Atomic Energy Commission
Washington, D. C. 20545

Director (1)
U. S. Weather Bureau
Attn: Librarian
Washington, D. C. 20235

Dr. Albert Miller (1)
Department of Meteorology
San Jose State College
San Jose, California 95114

Mrs. Francis L. Wheedon (1)
Army Research Office
3045 Columbia Pike
Arlington, Virginia 22201

Commander (1)
Air Force Cambridge Research Laboratories
Attn: CRXL
L. G. Hanscom Field
Bedford, Massachusetts

Harry Moses, Asso. Meteorologist (1)
Radiological Physics Division
Argonne National Laboratory
9700 S. Cass Avenue
Argonne, Illinois 60440

Defense Documentation Center (20)
Cameron Station
Alexandria, Virginia 22314

Office of U. S. Naval Weather Service (1)
U. S. Naval Air Station
Washington, D. C. 20390

Dr. Gerald Gill (1)
University of Michigan
Ann Arbor, Michigan 48103